NASA CR-431

BEAM ALIGNMENT TECHNIQUES BASED ON THE CURRENT MULTIPLICATION EFFECT IN PHOTOCONDUCTORS

By Raymond P. Borkowski, Aryeh H. Samuel,
and Daniel Grafstein

Distribution of this report is provided in the interest of information exchange. Responsibility for the contents resides in the author or organization that prepared it.

Prepared under Contract No. NAS 12-8 by
GENERAL PRECISION, INC.
Little Falls, N.J.

for Electronics Research Center

NATIONAL AERONAUTICS AND SPACE ADMINISTRATION

For sale by the Clearinghouse for Federal Scientific and Technical Information
Springfield, Virginia 22151 – Price $1.05

ABSTRACT

The multiplication effect in cadmium sulfide photoconductors, (a rise in photocurrent when light spots on opposing sides of a photo-conductor with two transparent electrodes are directed at exactly opposing spots) has been studied in a series of experiments which have confirmed its existence, defined many of its parametric dependencies, and permitted progress towards its explanation.

Photoconductive powders of cadmium sulfide and cadmium selenide were prepared and photoconductors of varying thickness were fabricated by casting, pressing, and spraying techniques. However, most measurements were made on commercial polycrystalline CdS cells, with one evaporated metallic and one conducting glass electrode. These cells had very high extinction coefficients ($\approx 10^3$ cm^{-1}). The following relationships were developed:

1. The wavelength dependence of the multiplication effect was determined. For any incident wavelength on one side, the multiplication factor (M) is greatest when the other wavelength is about 5200Å; the greatest value of M is obtained for the wavelength combination 5200Å and 6500Å.

2. When one beam is constant and the intensity of the other is varied, it is found that M passes through a maximum at moderate intensities; higher and lower light intensities give lower M.

3. The value of M is found to decrease as the electric field across the photo-conductor increases. There is a small change in M when polarity is reversed; it is greater when the metallic electrode is positive.

4. Attempts were made to measure the dependence of M on photo-conductor thickness, but these failed because of insufficient photoconductivity in the cells fabricated in this laboratory.

5. The dependence of M on the area of the light spot was measured in two modes; constant flux (defocused spot) and constant intensity. In both modes, a maximum M was found at intermediate spot sizes (0.5 - 1.0 mm) for most wavelength combinations.

6. Rise and decay times were measured for polycrystalline CdS cells (one-side illumination) and for single-crystal CdS cells (two-sided illumination, rise time only). In the latter, the occurrence of the multiplication effect was associated with a 40% reduction in rise time.

7. It was found that the value of M was not changed when the angle of incidence of light beams impinging on a given spot varied.

8. When light spots on opposite sides of a photoconductor are displaced linearly with respect to each other, M is reduced and reaches values near unity for displacements greater than 2mm. However, there is still some multiplication when the light spots are close but do not overlap.

9. No increase in current is observed when the spots are made to coincide on the same side of the photoconductor.

First steps have been made in constructing a model of the multiplication effect. A geometrical diffusion model, assuming the absorption of light near the surface of incidence, can account for the effects of displacement, field, spot area, and beam direction and for the observed change in rise time. A physical model, similar to those used to explain sensitization in CdS, is capable of explaining the wavelength dependence. A unified model has not been developed as yet.

A follow-on program is recommended. Among other objectives, the program will develop the material dependences of the effect. Rotating sector experiments are recommended in order to elucidate any time-dependent phenomena. A "breadboard" device utilizing the multiplication effect for beam alignment should be designed, fabricated and tested.

TABLE OF CONTENTS

		Page
	ABSTRACT	iii
I.	INDEX OF FIGURES AND PLATES	vi
	INDEX OF TABLES	viii
1.	INTRODUCTION	1
	1. Contract History	1
	2. The Multiplication Effect	1
	3. Topics of Investigation	2
II.	EXPERIMENTS AND RESULTS	3
	1. Preparation of Photoconductive Powders	3
	2. Fabrication of Photoconductive Cells	4
	a. Photosensitivity Measurements	4
	b. Testing of the Cells	6
	3. Parameter Dependences	9
	a. Wavelength	17
	b. Intensity	19
	c. Effect of Electric Field on M	25
	d. Thickness of Photoconductors	29
	e. Area of Light Spot	31
	f. Rise and Decay Times	33
	4. Geometrical Parameters	42
	a. Normal Versus Acute Illumination	42
	b. Effect of Relative Displacement of Light Spots	47
	c. Simultaneous Dual Beam Illumination of a Single Surface	48
	d. Effect of Varying Wavelength	48
	e. Effect of Varying Spot Size	48
III.	THEORY OF THE MULTIPLICATION EFFECT	51
	1. Introduction	51
	2. Geometrical Models of the Multiplication Effect	51
	a. First Crude Model	51
	b. Second Geometrical Model	55
	3. Physics of the Multiplication Effect	58
IV.	CONCLUSIONS AND RECOMMENDATIONS	60
	1. Conclusions	60
	2. Recommendations	62
	3. Recommended Program	63

Index of Figures and Plates

Figure		Page No.
1	Schematic Diagram of Experimental Arrangement	10
1A	Variation of Intensity of S_2 with Wavelength	12
1B	Intensity - Wavelength Distribution of Tungsten - Iodine Lamp (S_1)	13
2	Photocurrent versus Wavelength - Cell No. 3	14
3	Photocurrent versus Wavelength - Cell No. J-702	15
4	Wavelength Dependence of the Multiplication Effect	18
5	Variation in Photoresponse Curve for Several Intensities of Bias Illumination Opposite Side Illumination	20
5A	Multiplication Factor as a Function of Bias Photocurrent	22
6A	Photocurrent versus Electric Field for Single-Sided Illumination	26
6B	Photocurrent versus Electric Field for Dual Side Illumination;	
	Multiplication Factor as a Function of Electric Field	27
6C	Effect of Electric Field on M at Various Wavelength Combinations	28
7	Dark Current as a Function of Voltage for Reverse and Forward Bias	30
8	Effect of Spot Size on M (Defocusing Experiments)	32
Plate		
A - E	Variation of Photocurrent with Time for Various Wavelength Combinations for a Commercial Cell	36 - 38
	Plate A $\lambda = 5400\text{Å}$	
	Plate B $\lambda = 5350\text{Å}$	
	Plate C $\lambda = 5300\text{Å}$	
	Plate D $\lambda = 5200\text{Å}$	
	Plate E $\lambda = 6680\text{Å}$	
F	Variation of Photocurrent With Time for Single Crystal CdS Cell	40
G	Risetime Variation With Wavelength for Commercial Cell	41

Figure		Page No.
9	Beam Angle Variation. Schematic Diagram of Experimental Arrangement	43
10	Effect of Linear Displacement on M	49
11	Variation in Photoresponse Curve for Several Intensities of Bias Illumination - Same Side Illumination	50
12	Resistance and Carrier Concentration as a Function of Depth- Single Sided Illumination	52
13	Resistance and Carrier Concentration as a Function of Depth- Dual Side Illumination	52

Index of Tables

Table		Page No.
I	Composition of Photoconductive Powders	5
II	Description of Photocells	7
III	Test Data for Photocells	8
IV	Absorption Coefficients as a Function of Wavelength	11
V	Effect of Intensity on M	23 - 25
VI	Effect of Spot Size on M - Constant Intensity	34
VII	Rise and Decay Times of Photocurrents	39
VIII	Effect of Beam Angle on M	45 - 46
IX	Comparison of Actual and Calculated M	61

I. INTRODUCTION

1. Contract History

This is the first phase technical summary report on work done under National Aeronautics and Space Administration (NASA) Contract NAS 12-8, at the Aerospace Research Center of General Precision, Inc. The work reported on herein was conducted under the supervision of Dr. Daniel Grafstein, Head of the Chemistry Department. The principal investigator was Dr. Raymond P. Borkowski. Others who contributed to and supported the research effort were Dr. Aryeh H. Samuel, Mr. W. M. Block, and Mr. W. M. Benko.

The subject of investigation under Contract NAS 12-8 was the current multiplication effect in photoconductors which had been discovered at General Precision Aerospace about three years ago. In order to establish certain parameters of the effect, which might determine its relevance to NASA objectives, a four-man-month investigation was commissioned by the NASA Electronics Research Center. Experimental work began on May 27th, 1965 and continued until shortly before the due date of this report, which is October 15, 1965. The Contract Technical Director, at the NASA Electronics Research Center was Mr. Janis Bebris. The interest and assistance of Dr. Max Nagel, Acting Chief, Space Optics Laboratory, NASA Electronics Research Center is also gratefully acknowledged.

2. The Multiplication Effect

It was discovered that when two spots of light are directed at exactly opposite points on two opposing surfaces of a photoconductor an anomalously large photocurrent is achieved. If the photocurrents obtained by illuminating with either spot alone are i_1 and i_2, and the photocurrent obtained (at the same field) by illuminating with both spots is i_T, we find that the "multiplication factor" M, defined by:

$$M = \frac{i_T}{i_1 + i_2} \qquad (1)$$

is greater than one; in fact, values up to 100 have been observed.

It should be noted that a large value of M does not necessarily imply a large value of the photocurrent i_T, since M may also be large because the denominator of the ratio in equation 1 is small. Nevertheless, we believe that M is the most useful measure of the multiplication effect, since one will normally be interested in the ratio of the current obtained when the spots coincide (the "signal") to that obtained when they do not (the "noise").

3. Topics of Investigation

Under Contract NAS 12-8, the Aerospace Research Center planned to investigate the relative importance of each of the items listed below to an understanding of the phenomenon. Some aspects of all of the topics have been studied. The results have served to identify areas worthy of more intensive investigation.

Item 1. Prepare the following photoconductive materials

a. Doped cadmium selenide
b. Doped cadmium sulfide

Item 2. Utilizing doped cadmium sulfide prepared in Item 1, fabricate a series of uniform photocells of varying thickness up to several millimeters, and varying dopant and acceptor levels to achieve resistivity range and linear response range.

Item 3. Determine effect of following parameters on the magnitude of the multiplication factor:

a. Wavelength of incident light beams
b. Incident intensity
c. Applied field
d. Thickness of photoconductors
e. Area of light spot
f. Rise and decay times

Item 4. Compare the results of illumination by a single spot of light with that using two spot light sources illuminating opposite surfaces for the following combinations of parameters:

a. Varying direction of incident light beams illuminating exactly opposite points of the detector.
b. Varying position of incident light spot.
c. Varying position of light sources relative to electrodes.
d. Varying wavelength.
e. Varying spot size.

Item 5. Correlate results with external and internal parameters and develop the appropriate mathematical relationships.

II. EXPERIMENTS AND RESULTS

1. Preparation of Photoconductive Powders

In order to prepare photosensitive powders, that is powders whose conductivity increases when they are exposed to light, the usual procedure followed is one which is used for the preparation of phosphors. This preparation involves the deliberate and controlled incorporation of impurities (dopants) into the pure starting material, firing the mixture and grinding the mixture to insure optimum particle size. Preparation procedures differ only in the order and extent to which the above steps are carried out.

In the preparation of doped cadmium selenide and cadmium sulfide we have used two methods. The first method is a modification of a preparation described by R. H. Bube [1]. It was used for the preparation of doped cadmium sulfide only. This particular powder will henceforth be designated as Powder #1. The procedure used is as follows: First a mixture containing 14.5 grams of luminescent grade CdS powder (RCA), 3.6 grams of $CdCl_2.2\ 1/2H_2O$ (analytical reagent grade) and 2.8×10^{-3} grams of copper as cupric acetate, was prepared.

The mixture was slurried in distilled water and dried at 120°C. It was fired at 600°C in air for twenty minutes in a lightly covered silica crucible. The sample was then ground in an agate mortar and pestle. The yield was 16.8 grams. The sample was then washed free of chloride ion using de-ionized water. Any possible remaining Cl^- ion was removed by precipitating with $AgNO_3$. Then 0.025 gram of excess Cl^- ion was deliberately added to the mixture as $CdCl_2.2\ 1/2H_2O$. The resulting mixture was slurried and dried at 120°C. It was fired again at 675°C for twenty minutes in a lightly covered silica crucible. The powder was then ground. Then 0.5 gram of sulfur was added and the sample fired again at 500°C for twenty minutes. After the sample cooled, it was reground, placed into an open silica crucible and fired at 500°C for ten minutes under vacuum (0.1 - 0.5 mm Hg). Finally it was fired for ten minutes at 500°C in a nitrogen atmosphere. After this firing it was ground and used for the fabrication of the photodetector.

The other method which was utilized for the preparation of both doped cadmium sulfide and cadmium selenide (henceforth designated as Powder #2 and Powder #3, respectively) was described by earlier workers in this field [2, 3].

(1) R. H. Bube, J. Appl. Phys. 31, 2239 (1960).

(2) "Preparation and Properties of Cadmium Sulfide Photoconductors" J. Graham, F. Keller, H. Rogers, H. Shapiro and T. Spalvins ASTIA Document No. AD-148978. (1959).

(3) "Preparation and Performance of Sintered CdS Photoconductors" R.R. Billups, W. L. Gardner and M. D. Zimmerman ASTIA Document No. AD-212580.

First 10 cc of 0.0875 molar $CdCl_2.2\ 1/2H_2O$ (analytical reagent grade) and 15 cc of 0.0586 molar $CuCl_2.2H_2O$ (analytical reagent grade) were added to 15.0 gram of either 99.999% cadmium sulfide (Semi-Elements Inc. SE-9060) or cadmium selenide (Merck Electronic Grade). The slurry was ground in a ball mill for several hours. It was placed in an oven at 117°C and dried. The dry powder was reground, using a ball mill, after which the material was placed in an open silica crucible and fired in a preheated furnace at 625°C for three minutes. (There was a four and one half minute soaking time before the powder came to temperature). After the firing the powder was allowed to cool in a desiccator which was covered with a black cloth. This latter procedure is supposed to further increase the sensitivity of the powder. After cooling, an aqueous slurry of the powder was prepared, which was again ground by ball-milling (mullite pellets were used, as contact of the powder with metal is to be avoided). The slurry was dried, reground, and then stored in a desiccator. The pertinent data concerning the dopant concentrations are presented in Table 1. The amounts of doped CdS and CdSe recovered were 12.0 gram and 11.25 gram respectively. It should be mentioned that these data represent the initial concentrations of the dopants before any washing or firing procedures were carried out.

2. Fabrication of Photoconductive Cells

a. Photosensitivity Measurements

After preparing the doped powders it was necessary to check on their photosensitivity. Before this could be accomplished a sandwich-type cell had to be constructed. In these cells the powder was pressed between two conducting glass plates, each of which had an electrical lead attached. Only doped cadmium sulfide Powders #1 and #2 were used in the construction of these cells.

Several methods were tried to insure good interparticle contact in the powders. In one method, Dow Chemical Epoxy Resin #332 was added to the dry powder. After thoroughly mixing the resin and the powder, a hardener (dimethyl xylylene diamine) was then added. Once again the mixture was thoroughly stirred. An appropriate amount of the mixture was placed between the conducting glass plates and allowed to set. Because of the long setting time (approximately three hours) of this particular resin-hardener combination, it was rather easy to obtain the desired thickness and cross-sectional area.

Another method of preparing the cell consisted in making a pellet either from the dry powder or a powder-binder mixture. This was

TABLE I

COMPOSITION OF PHOTOCONDUCTIVE POWDERS

Powder	Host	Concentration (atom%)**			
		Cd*	S*	Cu	Cl
#1	CdS	15.7	15.6	0.044	32.3
#2	CdS	0.84	0	0.085	1.85
#3	CdSe	1.11	0	0.112	2.45

* excess

** concentration before firing and washing procedures undertaken

accomplished by placing an appropriate amount of the material in a pellet press, evacuating the chamber containing the powder and then applying pressure of 20,000 lbs/ in^2 to it. Discs of varying thicknesses and 1.24 cm^2 cross-sectional area were prepared in this manner.

In some cases the powder was treated further. After forming the pellet the disc was placed in a silica boat, which in turn was put into a 625°C furnace for fifteen minutes. The disc was exposed to air during the firing. This caused the surfaces of the pellet to be sintered.

A third method achieving good interparticle contact was to disperse the powder in acetone and then spray the dispersion on the conducting glass surface, using an artist's spray brush. The acetone was allowed to vaporize and the powder was then dried further in an oven at 110°C. Table II. lists all of the cells constructed, with comments about the method used to make them.

b. Testing of the Cells

The response to light of these photoconductors and the cells made from them was checked, using an externally applied field. The first step was to test the photosensitivity of the powders by measuring their resistances in the light and in the dark. Such preliminary measurements were carried out for Powders #1 and #2. Powder #1 was mulled in castor oil and squeezed between two conducting glass plates to a separation of approximately 10 microns. The powder was found to be photosensitive with a light-to-dark resistivity ratio of approximately 0.1.

A similar measurement was carried out on Powder #2 except that the pressed pellets between two conducting glass plates were used rather than a castor-oil mull of the powder. This measurement was performed on cells C and D, described in Table II.

The resistance of cell C in room light was 130,000 ohms, while in the dark, it was 720,000 ohms. The resistance of the cell was decreased to 50 ohms by sintering it at 625°C for fifteen minutes. However, the sintering process caused the cell to be insensitive to light as the resistance no longer changed when the cell was exposed to light.

The data obtained for these particular cells are summarized in Table III. The photocurrents given in Table III were obtained with full

TABLE II

DESCRIPTION OF PHOTOCELLS

Cell Designation	Powder	Thickness (mm)	Area (cm^2)	Comment
A	#1	0.25	1.60	Spray Cell
B	#1	0.26	1.24	Dry Powder
C	#2	0.32	1.24	Pellet unsintered
D	#2	0.32	1.24	Pellet sintered
E	#1	0.33	1.24	Pellet Powder & Binder
F	#1	0.67	2.02	Epoxy cell $\frac{\text{Powder}}{\text{Binder}} = 8$
G	#1	1.33	1.24	Pellet Powder & Binder
H	#1	2.55	1.24	Pellet Powder & Binder

TABLE III

TEST DATA FOR PHOTOCELLS

$\times 10^6$ (amps)

Cell	Volts	i_d	i_{pc}
A	45	0	No photoresponse
B	45	30	1
C	1.1	0.025	0.045
D	0.1	910	No photoresponse
E	45	.06	0.3
F	45	.25	11.25
G	45	0.1	1-2
H	45	0.14	No photoresponse

surface illumination using white light. No measurable photocurrent was observed when any of the cells were partially illuminated on either one or both sides with monochromatic light. The simultaneous partial illumination of opposite surfaces was carried out for several different wavelength combinations for each of these cells and no current multiplication effect was observed. Therefore, no useful information about the influence of photoconductor thickness on the multiplication phenomenon could be obtained with these cells. In addition to being insensitive, all the photocells constructed thus far were also very slow, having response times of the order of seconds.

3. Parameter Dependences

Before presenting the experimental data on parameter dependences obtained during the course of this work, a description of the general physical arrangement used to obtain these data will be given. The experimental procedure employed for the specialized experiments will be discussed separately. The spectral response characteristics of cadmium sulfide photocells are also discussed.

Figure 1 is a schematic diagram of the usual experimental arrangement utilized in these studies. Most of the experimental data were obtained for the commercial photoconductive cells. These cells were manufactured by Pioneer Electric and Research Corporation, Forest Park, Illinois and consisted of polycrystalline doped cadmium sulfide which was sandwiched between a Nesa conducting glass electrode and a transparent metallic electrode of either indium or gold. The cells were usually encapsulated to protect them from moisture and oxygen. The area of the photoconductor in these cells was approximately $1 cm^2$ and the thicknesses ranged from 50 to 75 microns.

The direction of illumination was perpendicular to each electrode and parallel to the direction of applied field for all of the studies reported here. The illuminated areas were defined by masks with circular apertures of known diameter or by a microscope objective-ocular combination. The area of the light spots employed ranged from $20 \times 10^{-6} cm^2$ (diameter = 51 microns) to $0.033\ cm^2$ (diameter = 2032 microns).

The applied electric field was varied by using a Helipot and the direction of the field could be changed with a reversing switch.

The wavelengths of both beams were controlled by separate monochromators, although interference filters were substituted occasionally for one of the monochromators.

Schematic Diagram of Experimental Arrangement

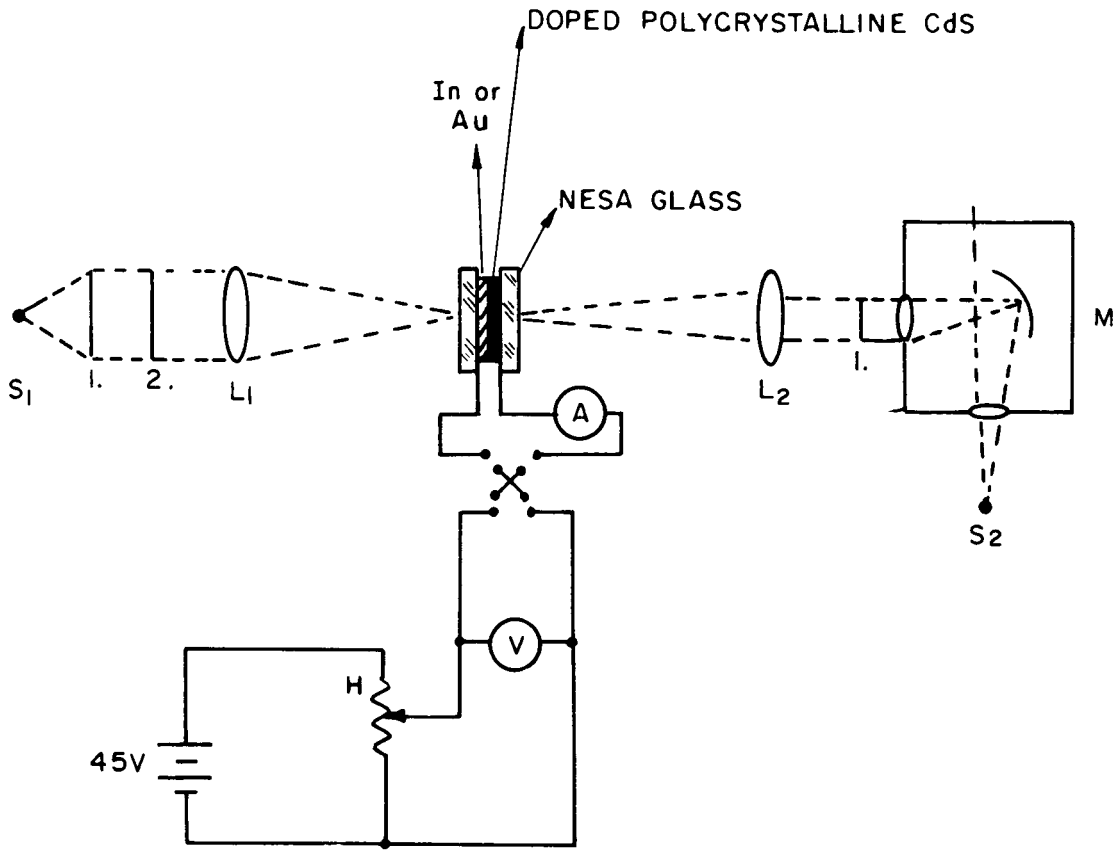

M	= monochromator
L_1 and L_2	= condensing lenses
1.	= H_2O filters
2.	= interference filters
A	= Keithley 150A Electrometer
V	= voltmeter
H	= helipot

FIGURE 1.

The intensity was varied by neutral density filters.

The light sources employed in this work varied also. Generally one beam (S_1 in Figure 1) was produced by a tungsten-iodine lamp and the other by a low voltage (6V), high amperage (18 amperes) concentrated filament incandescent lamp. For some experiments, S_1 was replaced by either a sodium vapor lamp or a lamp identical with S_2. Water filters were sometimes used to eliminate wavelengths in the infrared which could possibly heat the photoconductor. However, similar experimental results were obtained with or without these filters, so that in most instances they were not used.

Figure 1A gives the measured intensity versus wavelength relation for the tungsten incandescent filament lamp S_2. This was obtained using an RCA 1P29 phototube, and the phototube sensitivity characteristic has been allowed for. Figure 1B is the manufacturer's curve for the intensity versus wavelength relation of the tungsten-iodine lamp S_1.

Spectral response curves for two different polycrystalline cells are shown in Figure 2 and Figure 3 respectively. These cells exhibit maximum photosensitivity in the 6500-6700Å region and relatively low sensitivity in the wavelength region below 5500Å and above 7000Å. These spectral response curves are typical of the spectral response of all of the cells employed in this work.

The absorption coefficient of pure cadmium sulfide as a function of wavelength was determined. A few values of the absorption coefficient at different wavelengths are given in the table below.

TABLE IV

Absorption Coefficients (α) as a function of wavelength.
λ(Å)

λ(Å)	α(cm^{-1})
6500	29
5200	60
5100	90

FIGURE 1A. Variation of Intensity of S_2 with Wavelength.

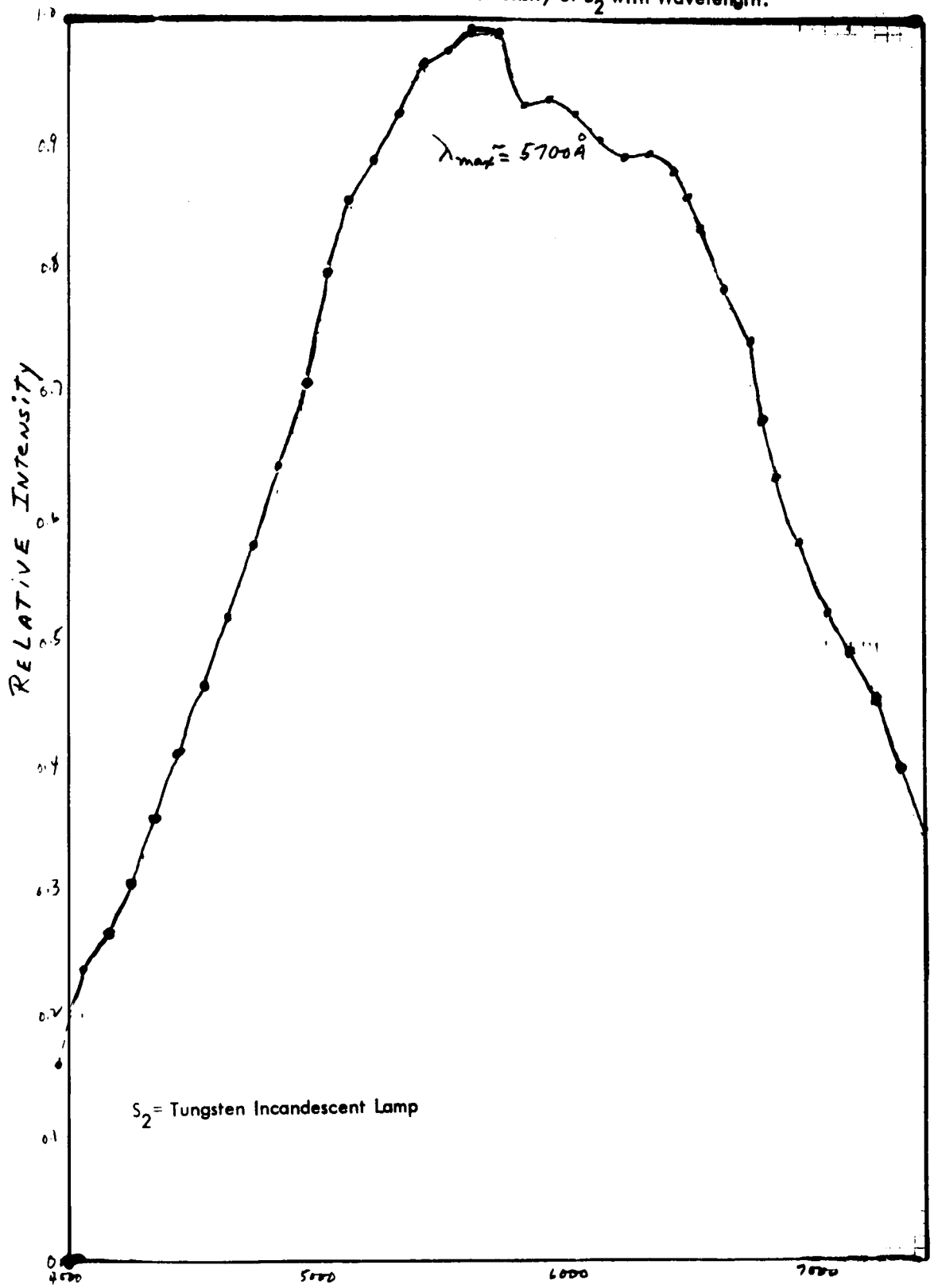

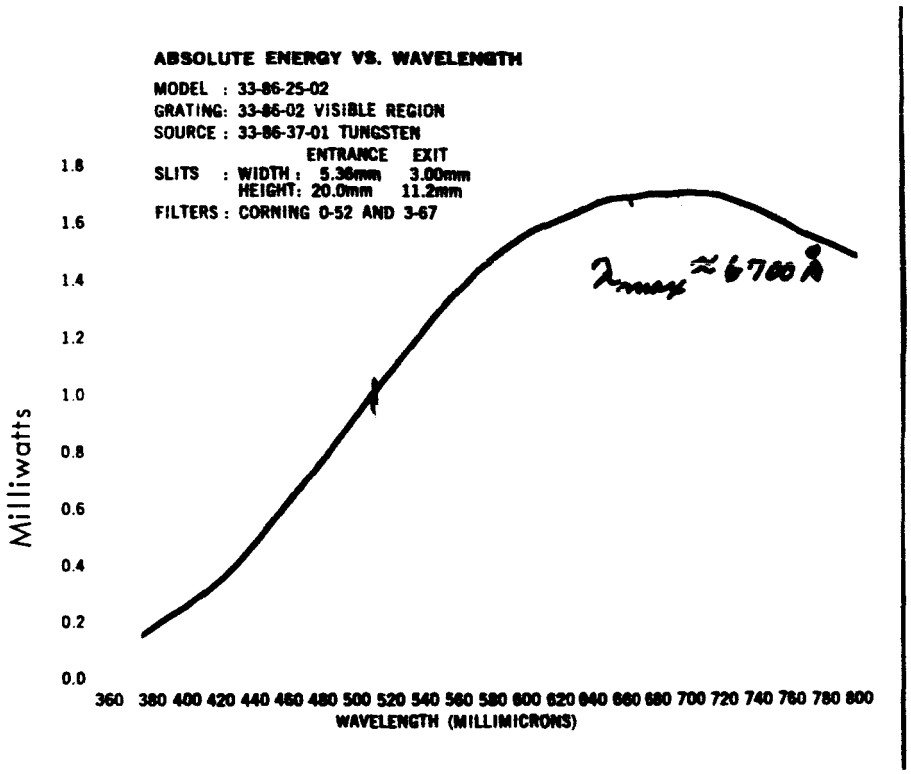

Intensity - Wavelength Distribution of Tungsten - Iodine Lamp (S_1).

FIGURE 1B.

FIGURE 2.

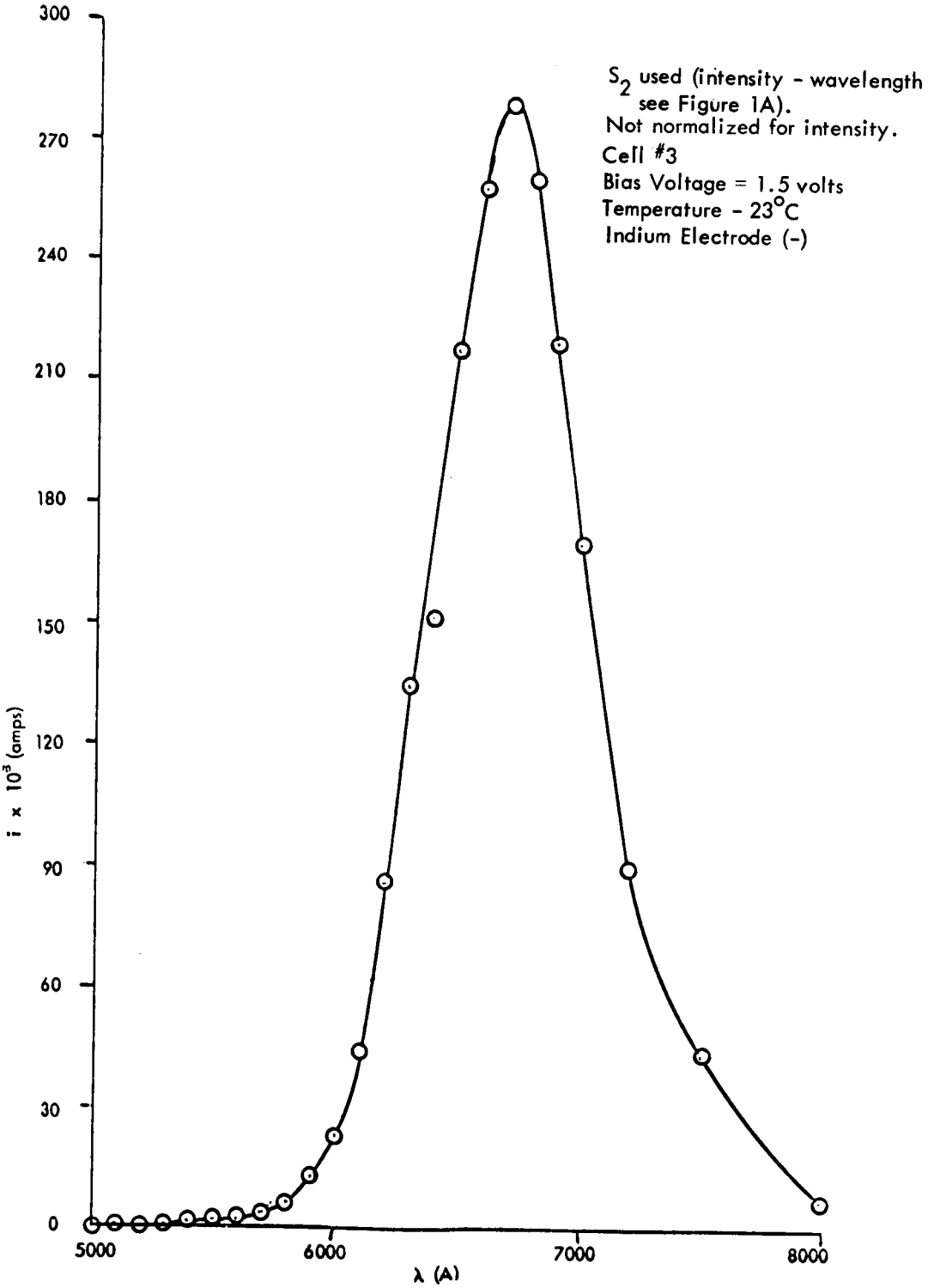

Photocurrent Versus Wavelength

Photocurrent versus Wavelength

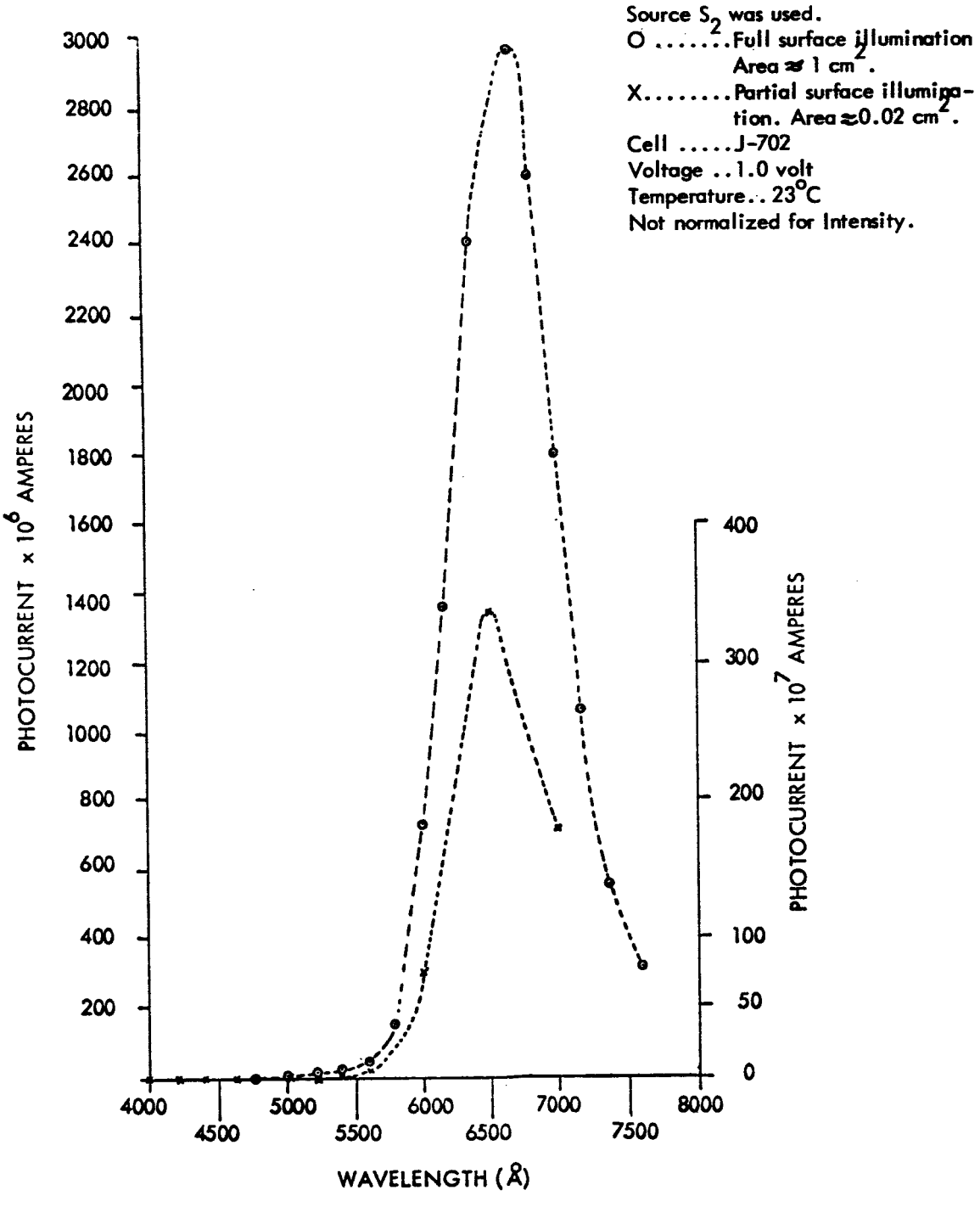

FIGURE 3

Thus, although the absorption of light by the cadmium sulfide is increasing as one goes to shorter wavelengths, the photosensitivity is decreasing. The decrease in the sensitivity with increasing absorption is attributable to the rapid recombination of electrons and holes at the surface. The absorption of the longer wavelengths is spread over the thickness of the photoconductor, whereas most of the absorption at the shorter wavelengths occurs near the surface.

The photoconductivity of pure cadmium sulfide is intrinsic and is due to transitions involving the main constituent atoms of the crystal. Most intrinsic materials have maximum photosensitivity of the wavelength corresponding to the minimum energy required to produce a free electron. For pure cadmium sulfide this would correspond to an energy of 2.43 e.v. (5100Å). Extrinsic materials are those in which photoconductivity is associated directly with impurities or with crystal imperfections such as vacancies. The absorption spectrum and the corresponding photoresponse spectrum are very similar to each other.

In the case of the polycrystalline cells, we know that we are dealing with an extrinsic material, since incorporation of impurities is necessary to make the polycrystalline cadmium sulfide photosensitive[1]. This explains why the wavelength of highest response has been shifted from 5100Å (pure CdS) to 6500Å. We would expect that there would also be a characteristic absorption band at 6500Å. Attempts were made to measure the absorption spectrum of the cells used, but high absorption of the composite cadmium sulfide layer and metallic electrode layer caused the transmission of light between 3500-7500Å to be unmeasurable (less than 0.1%) with our Beckman DK-2A Spectrophotometer. We conclude that the extinction coefficient of these cells is above 900 cm^{-1} throughout this wavelength range. Some of this absorption can be attributed to the evaporated metallic electrode; but not all, since we obtained photocurrents by illuminating through that layer.

In order to identify the impurities which were causing the photoconductivity in the region around 6500-6700Å, a few of these cells were subjected to analysis by X-ray diffraction, X-ray fluorescence and emission spectroscopy. The diffraction analysis confirmed hexagonal CdS was a major constituent and that it was highly polycrystalline. The X-ray fluorescence analysis showed that cadmium, iron and manganese were present in substantial amounts, with small amounts of copper, indium, zinc, zirconium and tin. The presence of these elements was also confirmed by emission spectroscopic analysis. The maximum in the spectral response curve at 6600Å would be expected in a 50% - 50% solid solution of cadmium sulfide and cadmium selenide, but no evidence for the presence

of selenium was found by any of these analytical methods. The maximum in the spectral response curve at 6600Å is, therefore, most probably due to impurities, probably copper and manganese.

Figure 3 illustrates the magnitudes of the photocurrents generated with full surface and partial surface illumination. When about one-fiftieth of the area is illuminated, the photocurrent is only 1/71 of that observed with full surface illumination, so that the amount of current generated is not precisely proportional to the area of illumination. The sensitivity does vary over the surface of the photocell and this non-uniformity could account for this relatively small deviation. This variation has been observed visually but details have not been recorded. In section 4b, we describe the effect of moving one beam across the photoconductor, while keeping the other fixed; and it may be of interest to note that in this experiment the photocurrent due to the fixed beam only varied from 7.8 to 10.8 micro amps($\pm$ 16%) while the photocurrent due only to the other beam, which was moved $\pm$ 2mm from coincidence, varied from 2.2 to 4.4 micro amps ($\pm$ 33%).

a. Wavelength

A typical wavelength dependence of the multiplication factor, M, is illustrated in Figures 4 and 5. In these experiments, the wavelength illuminating the metallic electrode was maintained constant (λ_1), while the wavelength illuminating the opposite surface through the glass electrode was varied (λ_2). In Figure 4 the multiplication factor is plotted as a function of the variable wavelength λ_2. A sharp maximum of M occurred for λ_2 of 5200-5300Å, with a maximum value of M near 85 occurring when the wavelength combination $\lambda_1 = 6640$Å and $\lambda_2 = 5200$Å was employed. The intensity of the two beams may be judged by the photocurrents produced by each beam separately. The photocurrent produced by the beam of variable wavelength λ_2 was in all cases very nearly that shown in the lower curve of Figure 3. The photocurrent produced by the beam of fixed wavelength λ_1 was:

$\lambda_1 = 4340$Å $\quad i_1 = 3\times10^{-10}$ amps

$\lambda_1 = 5020$Å $\quad i_1$ - less than 1×10^{-9} amp

$\lambda_1 = 5470$Å $\quad i_1 = 5\times10^{-10}$ amp

$\lambda_1 = 6640$Å $\quad i_1 = 1.13\times10^{-7}$ amp

FIGURE 4.

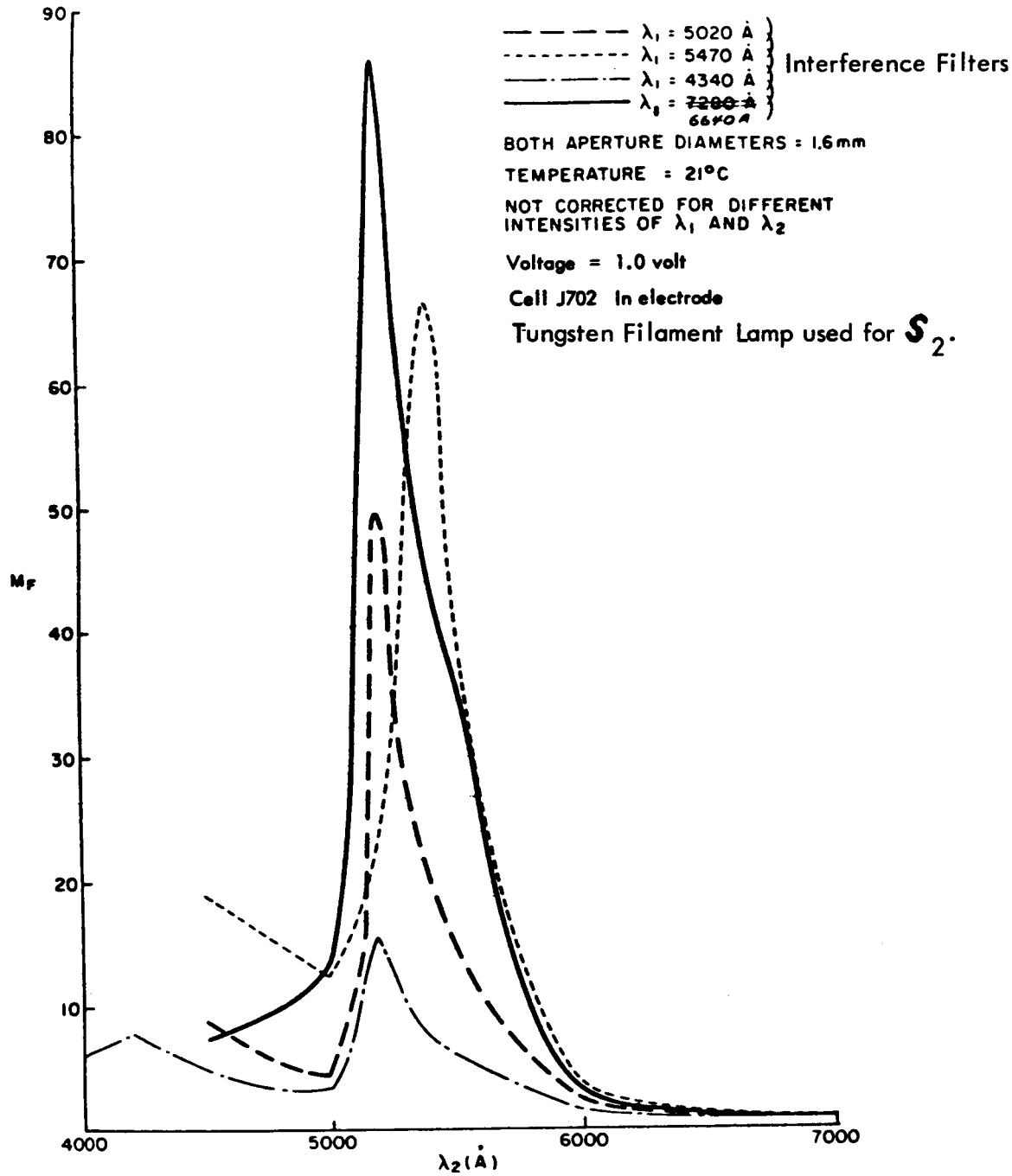

WAVELENGTH DEPENDENCE OF THE MULTIPLICATION EFFECT

A comparison between the intensities of the incident beams is possible only for the last case, in which the photocurrent from beam 1 is 0.38% of that produced by beam 2 at the same wavelength. Since the light sources are similar, this ratio is probably similar at other values of λ_1. The low intensity of beam 1 is attributed to the absorption of light by the metallic electrode.

In Figure 5 the results are presented in a different fashion. In these experiments the wavelength of one of the light beams, which we shall call the "bias" beam, was fixed at 6550Å, and the wavelength of the beam illuminating the other side of the cell was varied from 4000 to 7000Å. The intensity of the bias source was varied by varying the slit opening of the bias monochromator. The lowest curve, of Figure 5 represents the response of the cell for varying wavelength when the intensity of the bias source is zero (i.e. with single side illumination). It represents the spectral response of this particular cell, which was shown in Figure 3. Note the relatively insensitive region around 5100Å and the maximum in the response around 6500Å. Each subsequent curve represents the response of the cell with both light sources on. The numbers above each curve are proportional to the intensity of the bias source; they are the photocurrent obtained with single-side illumination at that particular value of the bias intensity with the other beam turned off. This type of representation shows very clearly that a positive non-additivity of the photocurrent has taken place, most markedly at the wavelength given by the vertical dotted line (5180Å). This confirms the results illustrated in Figure 4, obtained by another method. In addition the data in Figure 5 also show that no multiplication occurs when the variable excitation wavelength exceeds 6000Å.

It is quite obvious from the data presented that the multiplication phenomenon is strongly dependent on the combination of wavelengths used. In fact, one of the wavelengths required to obtain an optimum effect is one to which the photoconductor is rather insensitive, namely 5200Å.

b. Intensity

The photocurrent produced in cadmium sulfide is known to be proportional to a power of the incident light intensity, that is ($i = kl^n$), where the exponent n can have values ranging from 0.5 to 3.0 depending on the temperature and the incident intensity. Thus it was necessary to establish the relationship between photocurrent and incident intensity for one-sided illumination of the commercial cells in order to determine whether a sub-linear or supralinear dependency existed for the intensities

FIGURE 5

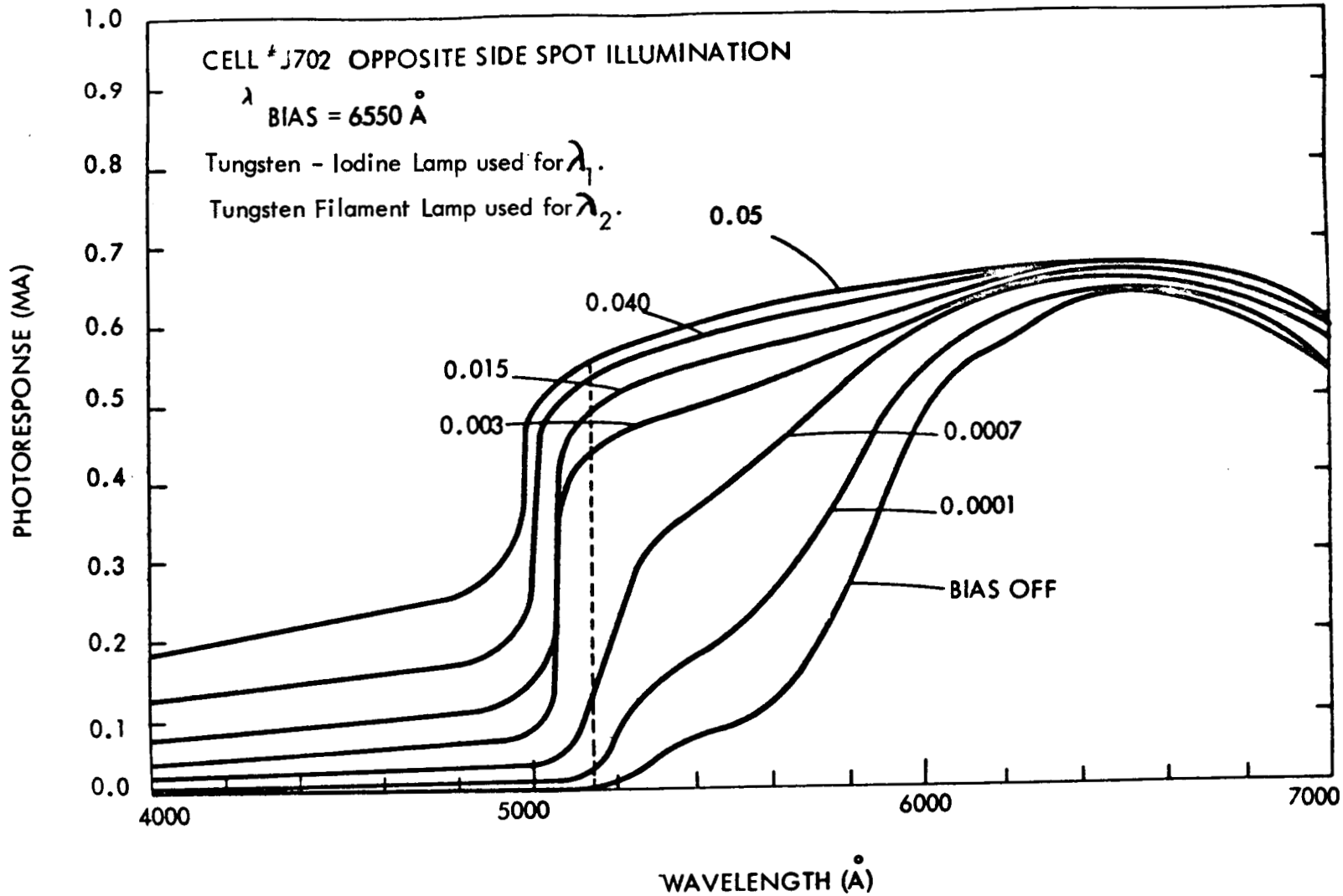

VARIATION IN PHOTORESPONSE CURVE FOR SEVERAL INTENSITIES OF BIAS ILLUMINATION
(NUMBERS OVER EACH CURVE GIVE CURRENT (MA) DUE TO BIAS ILLUMINATION ALONE)

used in the multiplication studies. These experiments were performed over a range of intensities extending from 0.75×10^{13} to 3×10^{16} quanta/cm^2-sec, using single-surface illumination. An approximately linear relationship ($I = kI^{0.8}$) was obtained. This work was done before the inception of the research effort reported on here, and details are not available. It is cited here only to show that superlinearity does not occur in these systems.

The data presented in Figure 5 illustrates also the influence of intensity on the multiplication factor. In Figure 5 the relative intensity of the variable-wavelength beam and the bias beam can be obtained by comparing the photocurrent obtained when the former is at 6550Å and the latter is off (0.63 ma) with the currents obtained using only the bias beams (0.0001 to 0.05 ma). It is seen that the bias beam varies in intensity from 0.016% to 8% of the intensity of the variable wavelength beam. Figure 5A shows the variation of M as the "bias" intensity is varied. These values were obtained from Figure 5 which represents a recorder tracing.

The data tabulated in Tables VA - VD also show the behavior of M as the intensity of one of the sources is varied for other cells and the other experimental conditions.

In these experiments one of the sources was unfiltered polychromatic white light from a tungsten arc, whose intensity was varied with neutral density filters. The other source was a beam of constant intensity, monochromatized by interference filters (VA to VC) or a sodium lamp(VD).

The trend is similar to that illustrated in Figure 5. The occurrence of a maximum M at intermediate values of the intensity appears to be quite general. This behavior can be understood by looking at the expression for the multiplication factor (Eq. 1).

The intensity I_2 of one of the beams is maintained constant so that M becomes $i_T/(k + i_1)$ (where k is constant). Decreasing I_1 causes a decrease in both i_1 and i_T. However, the change in the value of M would depend on the rate of change of i_T and i_1 respectively. When

$\frac{d\ln i_T}{dI_1}$ is greater than $\frac{d\ln(k + i_1)}{dI_1}$, M will increase with increasing I_1; and vice versa. Eventually as $i_1 \to 0$, $i_T \to k$, and M should approach unity. The maximum multiplication factor is attained when

FIGURE 5A. MULTIPLICATION FACTOR AS A FUNCTION OF BIAS PHOTOCURRENT.

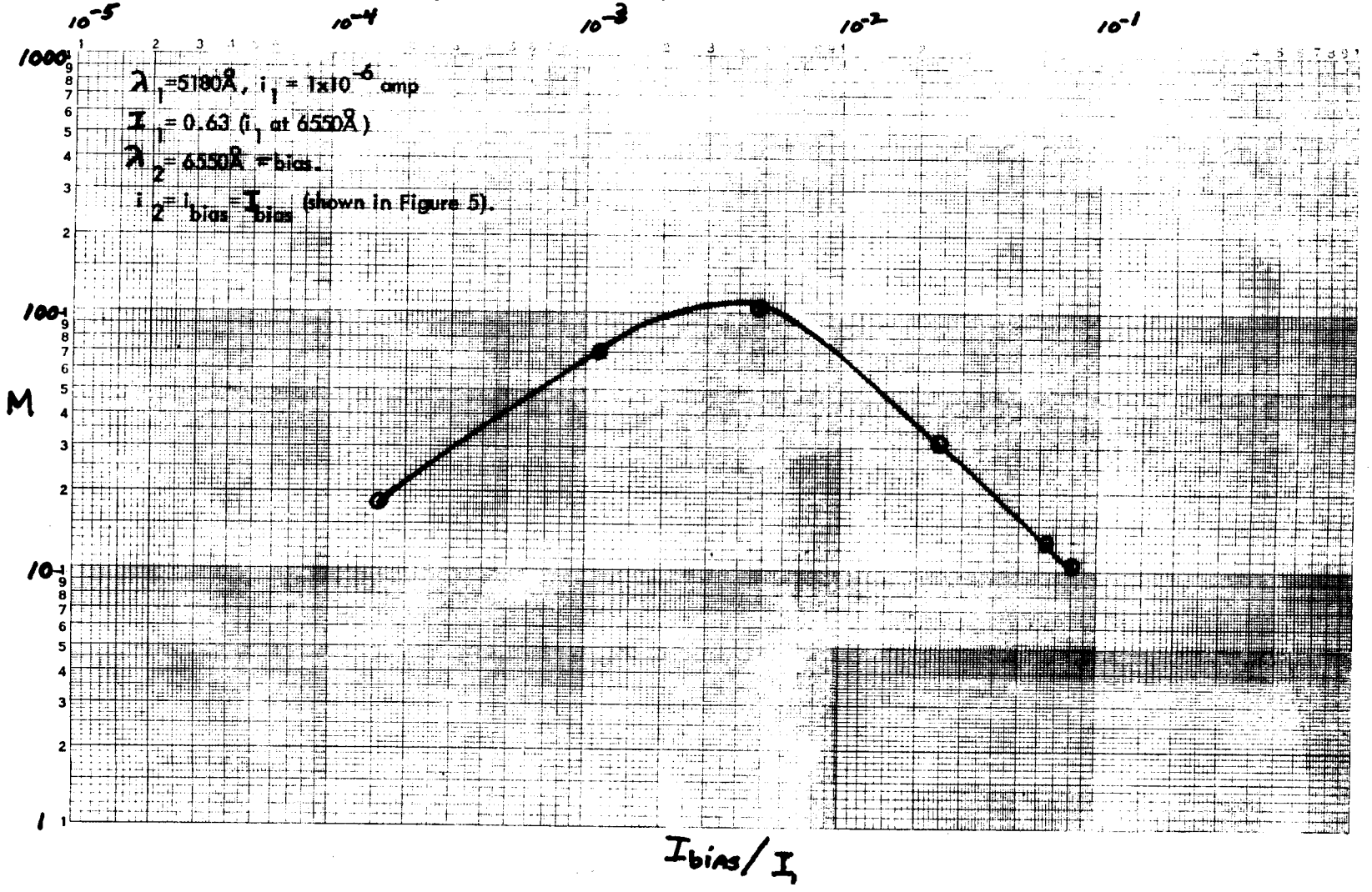

$\frac{d\ln i_T}{dI_1} = \frac{d\ln(k + i_1)}{dI_1}$. The intensity at which this maximum is reached varies. In the experiments described in Table V - D the maximum was not reached even at the lowest intensities used.

TABLE V

Effect of Intensity on M*

A.) Cell #1 — Au electrode (÷)

V = 1.0 volt — Mask Diameter = 1.58 mm

$\lambda_2 = 4340\text{Å}$

I_1, Relative Intensity, %	Amperes x 10^6			
λ_1 (Full Arc = 100%)	i_1	i_2	i_T	M
100	271	6.8	741	2.68
63.5	201	6.2	661	3.20
25.1	107	6.2	510	4.51
10.0	56.8	6.8	366	5.58
0.1	0.60	6.4	20.8	3.00

* S_1 is an unfiltered tungsten lamp illuminating the left-hand photoconductor surface through the metallic electrode and giving photocurrent i_1. S_2 is a monochromatic beam of wavelength λ_2 illuminating the right-hand photoconductor surface through the glass electrode and giving photocurrent i_2. The intensity of S_1 is varied by neutral density filters.

TABLE V - Continued

B.) Cell J-780
V = 1.5 volts
λ_2 = 5470Å

In Electrode (+)
Mask Diameter = 0.84 mm

I_1, Relative Intensity, % λ_1(Full Arc = 100%)	Amperes x 10^6 i_1	i_2	i_T	M
100	140	240	480	1.26
79.5	100	235	430	1.28
63.5	96	240	420	1.25
15.8	21.2	240	305	1.17
10	9.6	235	285	1.17
1	0.42	220	245	1.11
0.1	0.02	240	240	1.00

C.) Cell J-780
V = 1.5 volts
λ_2 = 4340Å

In Electrode (+)
Mask Diameter = 0.84 mm

I_1 Relative intensity, % λ_1(Full Arc = 100%)	Amperes x 10^6 i_1	i_2	i_T	M
100	139.5	7.0	210	1.43
79.5	119	6.5	179	1.43
63.5	97	6.9	154	1.48
15.8	23.5	6.9	48	1.58
10	15.4	6.9	35	1.58
1	0.65	7.2	9.0	1.15
0.1	0.00	7.15	7.15	1.0

D.) Cell J-686 — In Electrode (+)
V = 1.0 Volt — Na Vapor Lamp
λ_2 = 5889-95Å

I_1 Relative Intensity, %	Amperes x 10^6			
λ_1 (Full Arc = 100%)	i_1	i_2	i_T	M
100	1070	8.6	1065	0.99
63.5	970	10	990	1.01
10	690	10.6	800	1.14
1.0	135	10.0	258	1.78
0.1	11.0	8.2	48	2.50

c. Effect of Electric Field on M

Studies of the dependence of M on applied field showed that M generally decreased with increasing field to a constant value. An illustration of this is shown in Figure 6B where a forty-fold increase in field from 100 to 4000 volts/cm caused M to decrease from 6.7 to 1.8; it then remained constant for fields as high as 8000 volts/cm. Additional data showing the influence of the electric field on M are illustrated in Figure 6C for another cell at different wavelength combinations, indicating that this is the general behavior of M with varying electric field.

An analysis similar to the one given for the influence of the intensity (item 4b) can be employed. Each photocurrent, i_1, i_2, and i_T increases with increasing electric field in the manner shown in Figures 6A and 6B. The behavior is not linear over the entire range of field utilized. In order for M to decrease with increasing field the fractional increase in the total photocurrent with field

$\frac{1}{i_T} \frac{di_T}{dE}$ had to be less than the sum of the fractional increases in the individual photocurrents $\frac{1}{i_1} \frac{di_1}{dE} + \frac{1}{i_2} \frac{di_2}{dE}$. The numerator i_T would thus be increasing by a smaller factor than the denominator $(i_1 + i_2)$, producing a decrease in the ratio, i.e. M.

FIGURE 6A

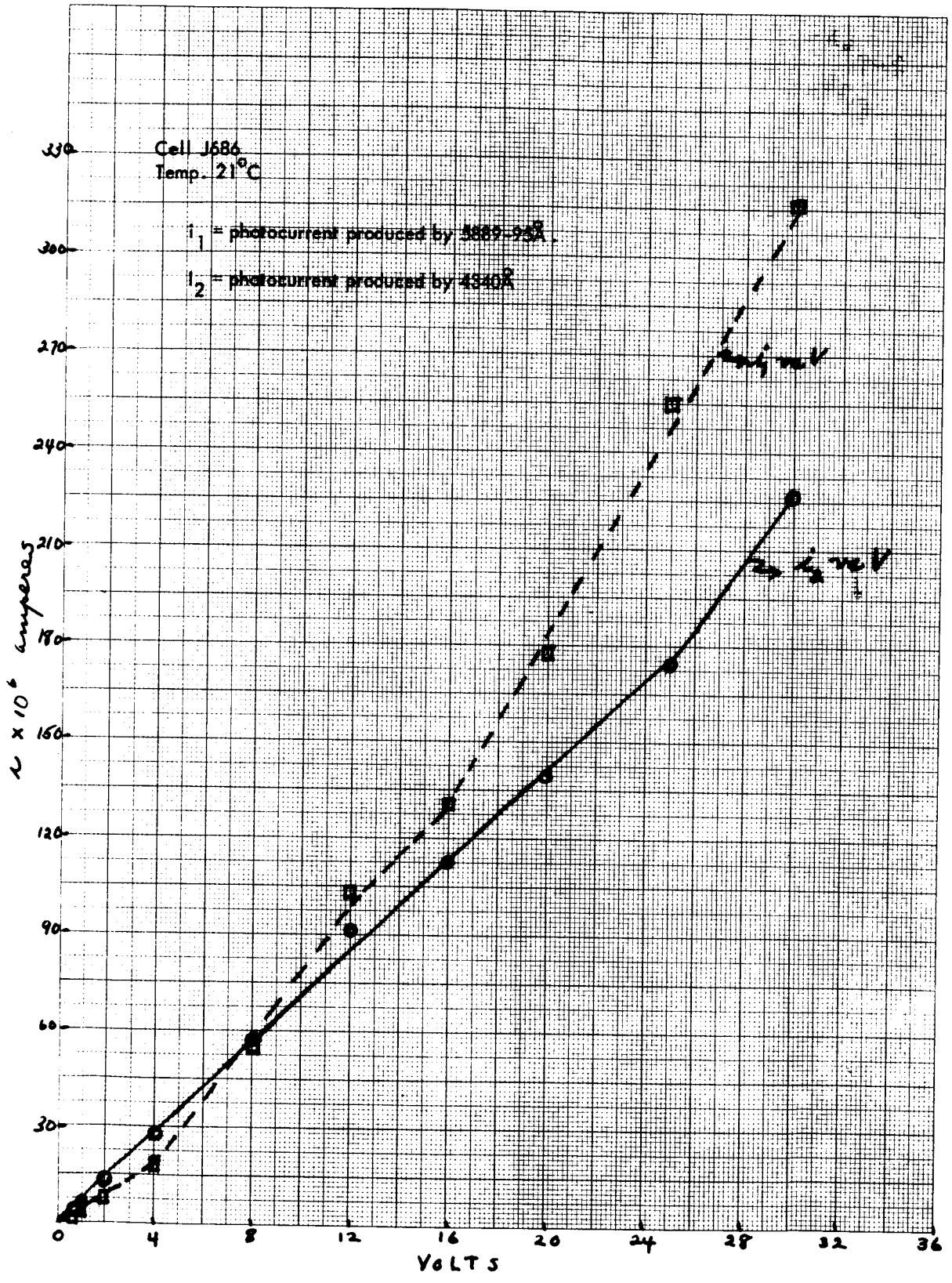
Cell J686
Temp. 21°C
i_1 = photocurrent produced by 3889-95Å.
i_2 = photocurrent produced by 4340Å
330
300
270
240
210
180
150
120
90
60
30
i x 10⁶ amperes
0
4
8
12
16
20
24
28
32
36
VOLTS

FIGURE 6B

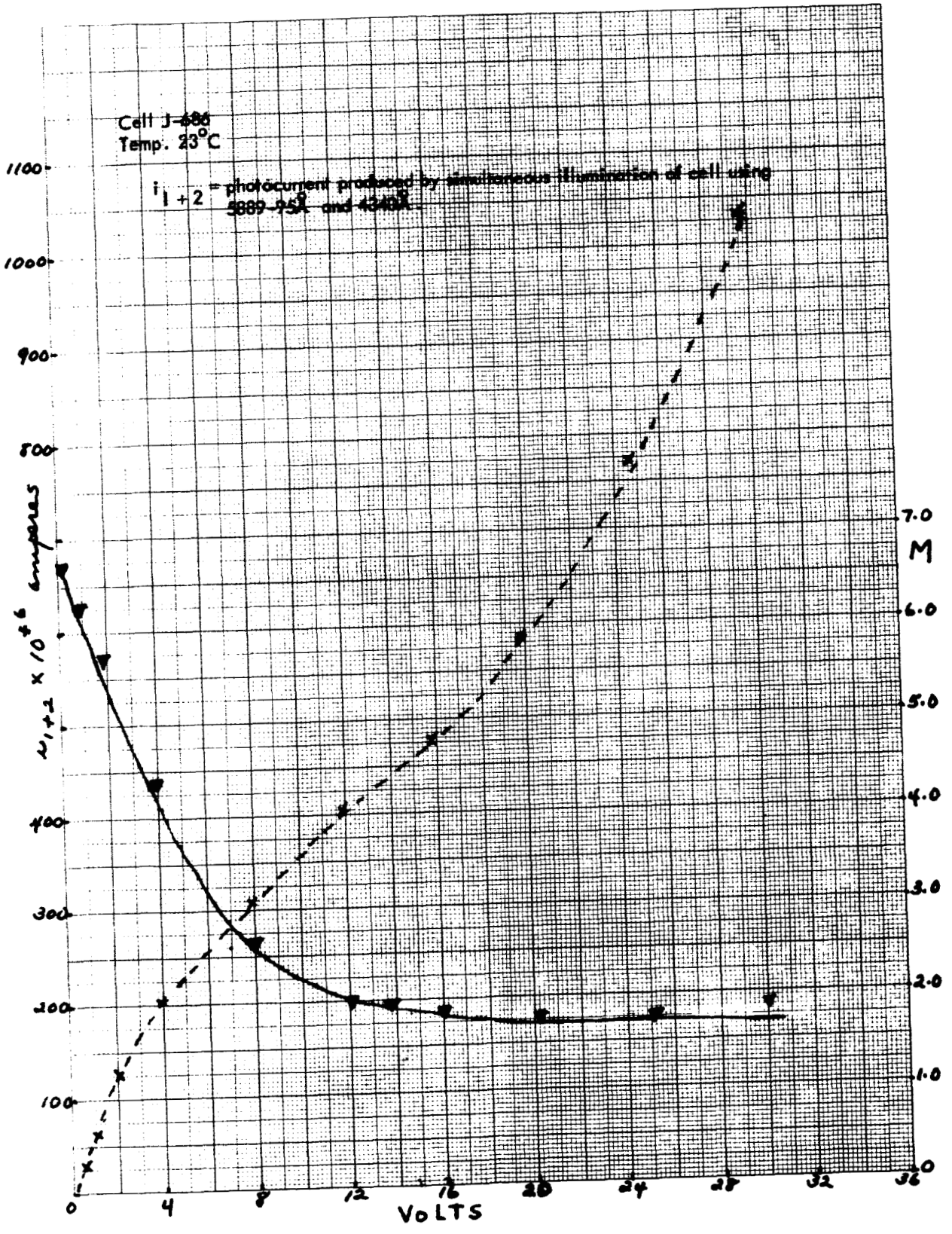
Cell J-686
Temp. 23°C
i_{1+2} = photocurrent produced by simultaneous illumination of cell using 5889-95Å and 4340Å
1100
1000
900
800
400
300
200
100
0
4
8
12
16
20
24
28
32
36
VOLTS
i_{1+2} x 10^{+6} amperes
7.0
M
6.0
5.0
4.0
3.0
2.0
1.0
0

FIGURE 6C. EFFECT OF ELECTRIC FIELD (E) ON M AT VARIOUS WAVELENGTH COMBINATIONS.

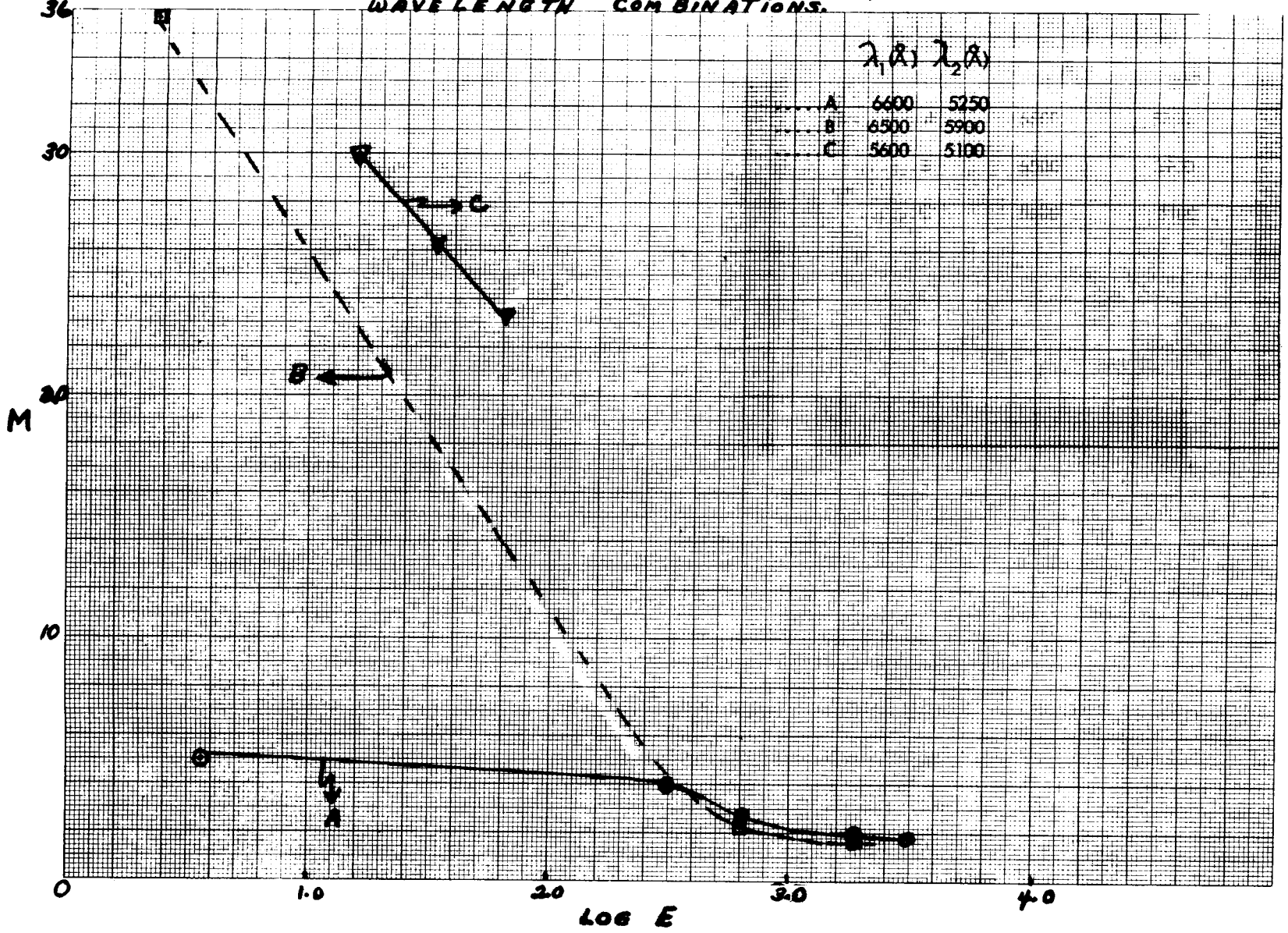

In addition to studying the effect of the magnitude of the electric field, we also investigated the effect of varying the direction of field (polarity). Because the electroces in our cells were applied to the large surfaces of the photoconductor disks, the applied electric field was always normal to these surfaces; however, the direction of the field could be reversed by a reversing switch. We cefine a direction of forward polarity (F) in which the metallic electrode was positive, i.e. connected to the positive terminal of the battery, and reverse polarity (R) when it was negative. It was determined that the multiplication factor was always greater under forward polarity. However, the ratio of "forward" M to "reverse" M for all of the cells that were studied was never greater than 3 and in most instances it was less than 2.

An attempt was made to determine why such polarity dependence should occur. First of all, a current-voltage curve of one of the cells having an indium electrode was obtained under room illumination for both the forward and reverse field direction. The results are given in Figure 7. The data indicate that the current is a linear function of the voltage in both the forward and reverse directions of field, showing that the cell is ohmic. However, the slope in the forward direction is smaller than the slope in the reverse direction. This means that, for any particular value of the field, the currents in the reverse direction would be larger than those in the forward direction by the ratio of the slopes (m_R/m_F) which for the data given in Figure 7 would be 1.38. On the other hand, little or no dependence of i_T on the field direction was found. Based on this analysis, the denominator of the ratio

$\frac{i_T}{i_1+i_2}$ should be greater and M should be about 1.38 times smaller in the reverse direction. Thus we attribute the effect of polarity on M as due to the asymmetry of the current-voltage relationship for the particular cell.

d. Thickness of Photoconductors

Commercial photoconductive cells of large thickness or known variations in thickness were not available. Thus, the characterization of the thickness parameter required us to attempt to fabricate our own cells with thicknesses up to several millimeters. Under items 1 and 2 we have described the production of doped cadmium sulfide and selenide and the fabrication of cells in the desired thickness from these powders. It is unfortunate that the photoconductive properties of these large cells were not sufficient to enable us to develop the desired relationship. While these thick cells showed slightly higher current when

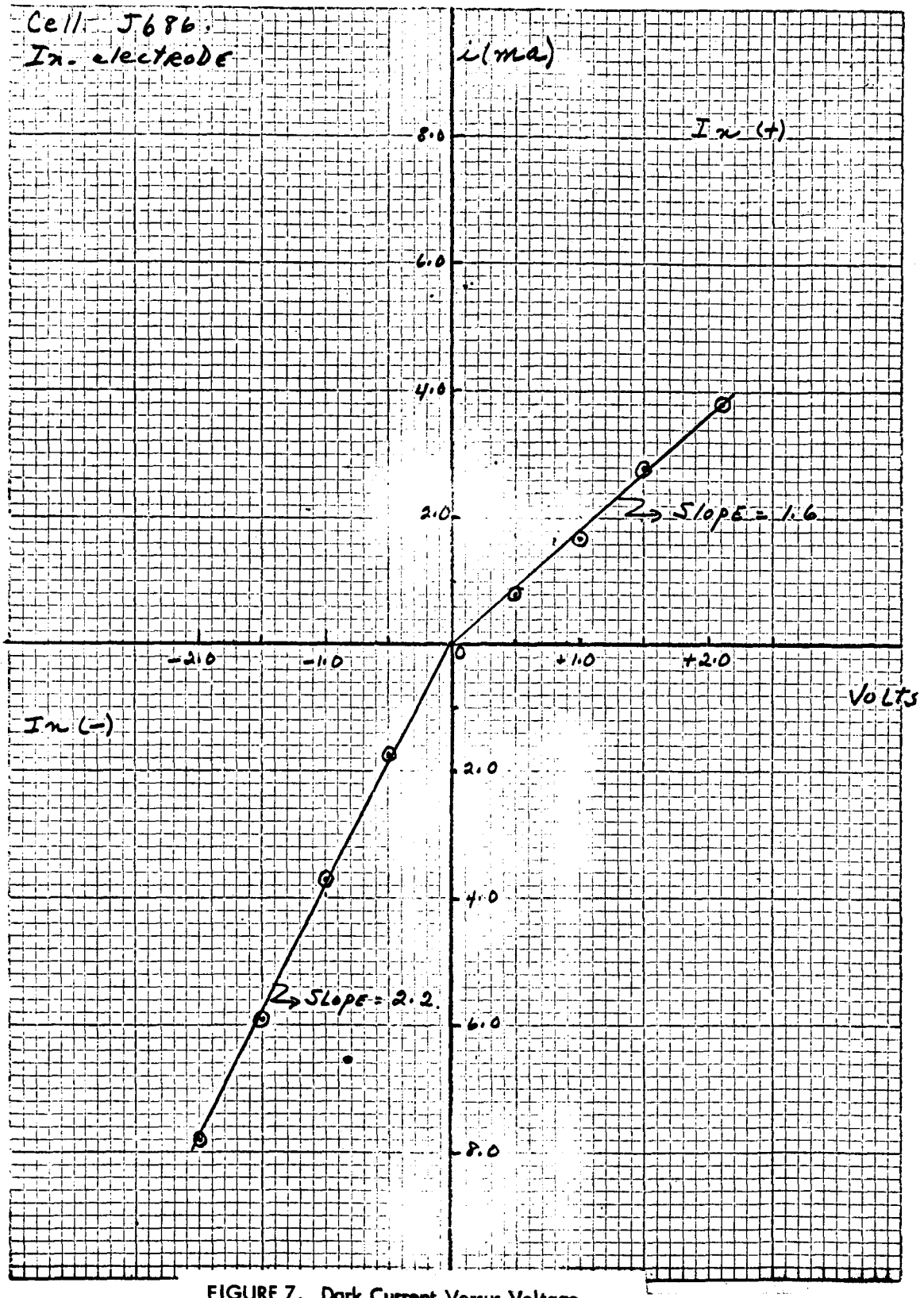

FIGURE 7. Dark Current Versus Voltage.

illuminated full-face than in the dark, spot illumination produced no measurable increase in current over dark current. The same result was observed when directly opposite spots were applied to both surfaces. The value of the multiplication factor in these particular cells is therefore indeterminate; it is not proper to assume that the effect is absent. A further definition of the effect of thickness must await the fabrication or purchase of more sensitive photoconductors having the desired thickness parameters.

e. Area of Light Spot

In the first of two series of experiments in which light spot area was varied, the spots were produced by focusing the light from each monochromator with a microscope objective-ocular lens combination to position the spots. Then the glass plate was replaced by the photoconductor. In these experiments the area of the right spot was constant while the area of the left spot (illuminating the indium electrode) was increased by defocusing the ocular lens on that side. The total light flux was maintained constant whereas the intensity was varied.

In the second series of experiments masks were employed to produce spots of light. In order to insure coincidence of the light spots, the masks were made in matched pairs, so that the spot sizes on both sides were always the same. The light beam from each monochromator was defocused and allowed to cover each mask completely. Thus, the incident intensity per unit area was maintained constant. The areas of the circular apertures ranged from $2.04 \times 10^{-5} cm^2$ to $3.24 \times 10^{-2} cm^2$.

The influence of spot size on M by defocusing one of the light spots is illustrated in Figure 8 for four different wavelength combinations. The spot size increases with increasing Q, which is the distance that the ocular lens is moved out of focus. Since the defocused spot has no sharp boundary, this is the best parameter that can be used. The variations in M are very similar to the trend noted with intensity in that M increases with decreasing spot size, reaches a maximum value, and then decreases with further increase in spot size. It would therefore be reasonable to attribute this variation in M to some specific spot size effect.

Nevertheless, we note that the maximum value of M for all four wavelength combinations is achieved at the same value of the defocusing parameter Q (0.7mm). At this point, in all cases i_1 has dropped considerably, while i_T has dropped very little. This may be a coincidence;

FIGURE 8.

Effect of Spot Size on M Defocusing Experiments

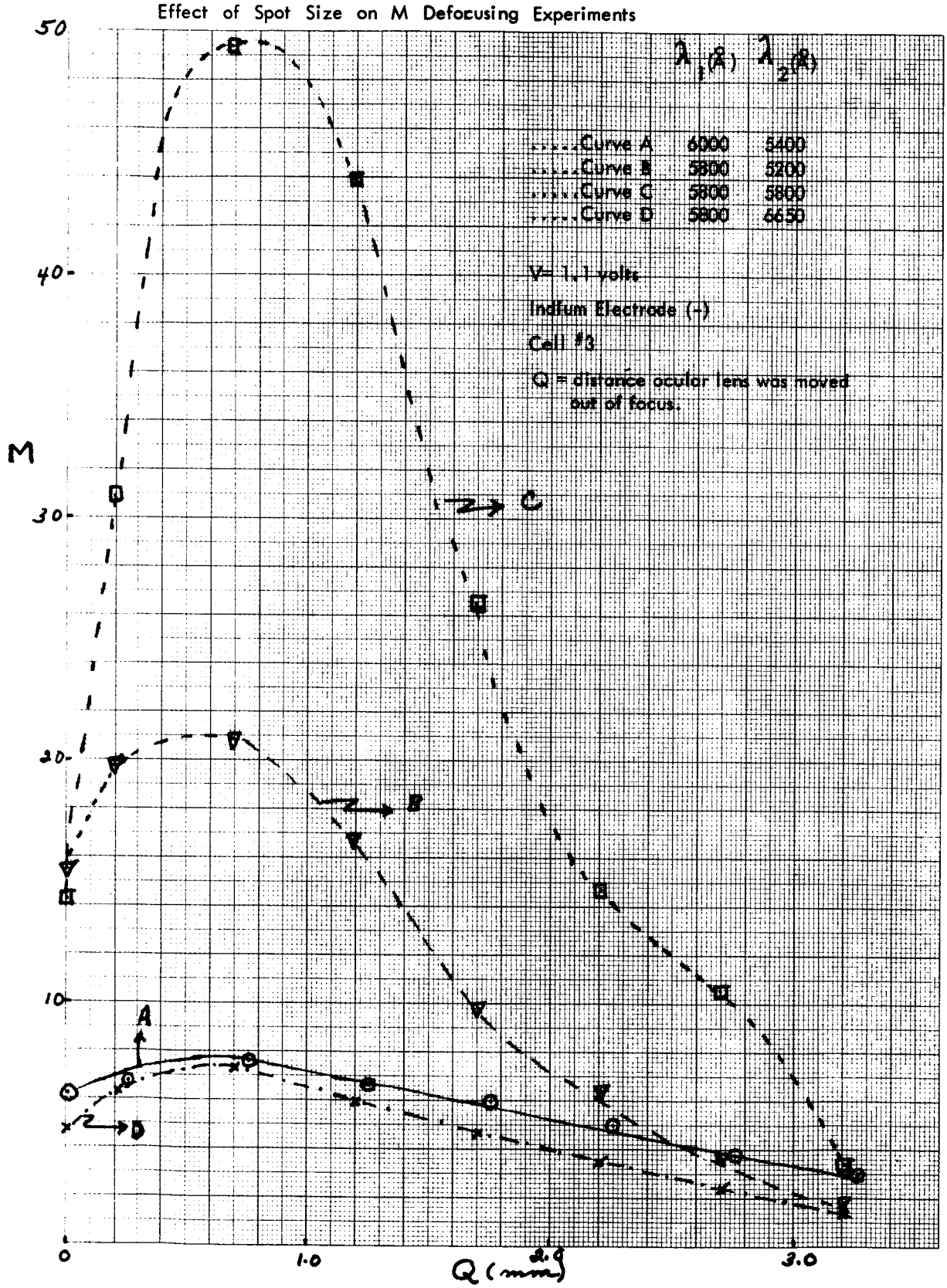

but the results could also be interpreted to mean that the spot size corresponding to Q=0.7mm is the largest to permit efficient inter-diffusion and interaction of charge carriers.

The results of the spot size experiments using masks are given in Table VI. Here the intensity is constant and therefore variations in M cannot be attributable to intensity. These results show that M is a maximum for a spot area of $20 \times 10^{-3} cm^2$, except for the wavelength combination $\lambda_1 = \lambda_2 = 5000\text{Å}$. In the first experiment, however, the measured currents were very low especially for the smaller spot areas. This possibly could be correlated with the fact that no maximum in M was observed. The maximum observed in the other experiments, at an aperture diameter of 0.51 mm, may again correspond to some critical distance.

f. Rise and Decay Times

Measurements of rise and decay times were made for the following situations:

A polycrystalline cell with one-side illumination.

A single-crystal cell with two-side illumination.

The time constants (response times) of the commercial cells were specified by the manufacturer to be in the range 10-20 milliseconds. This corresponds to the time it takes the photoconductor to achieve a photocurrent of one-half its steady-state photocurrent when the background illumination is 10^{13} quanta/sec-cm^2 or 50 foot-candles. Time constants or response times depend on the level of the background illumination, usually decreasing with increasing light intensity.

The behavior is consistent with the photocurrent varying with a power of the intensity which is less than unity. However, for a cell in which the photocurrent increases linearly with intensity, the response time should be a constant, independent of the intensity. For the commercial cells $i = kI^{0.8}$ for the range 0.75×10^{12} to 3×10^{15} quanta/cm^2-sec. Over this intensity range the response time should decrease, and it has been determined, using white light, that when the intensity was changed from 10^{11} quanta/cm^2 -sec to 10^{13} quanta/cm^2-sec. the time constant decreased from 1 second to 10^{-3} second.

For intensities above 10^{13} quanta/cm^2-sec, the photocurrent is proportional to the incident intensity, and a constant rise time is found.

TABLE VI

EFFECT OF SPOT SIZE ON M - CONSTANT INTENSITY

Cell #4 - Indium electrode (-)
Voltage = 1.1 volts

Maxima for each wavelength combination are underlined

λ_1(Å)	λ_2(Å)		$(A_1 = A_2) \times 10^6 cm^2$					
			20.4	248	856	2036	8100	32,350
5000	5000		1.0	1.31	2.66	2.77	5.65	<u>9.2</u>
5200	5200		1.81	1.53	2.58	<u>5.76</u>	4.9	3.0
5800	5200	M	1.20	1.11	1.61	<u>2.60</u>	1.87	1.17
5800	5800		1.23	1.34	1.47	<u>2.26</u>	1.56	*
5800	6650		1.03	1.02	1.23	<u>1.47</u>	1.21	*
6000	5400		1.02	1.10	1.52	<u>1.95</u>	1.56	*
6650	5800		1.13	1.04	1.26	<u>1.51</u>	1.21	*

* not determined

A_1 = area of left light spot

A_2 = area of right light spot

In this case, the rise and decay curves of the photocurrent are exponential:

$$\text{Rise: } i/i_0 = k\,(1 - \exp(-at))$$

$$\text{Decay: } i/i_0 = k' \exp(-at)$$

where i_0 is the steady-state current under illumination. These expressions have been used to obtain the rise and fall times (1/a) from the oscilloscope traces.

We measured rise and decay times on the commercial cell J-702, which had an indium electrode. The other electrode was a masked transparent conducting glass electrode through which the light was directed. A bias of + 0.5 or - 0.5 volt was applied. The results of these experiments are shown in Plates A through E. Each of these photographs shows the rise of photocurrent as a function of time of illumination by light of a different wavelength. In each of the top two quadrants of each plate the ascending curve represents the rise portion and the descending trace represents the decay time with the conducting glass electrode as the cathode (-electrode). The bottom two quadrants represent the rise and decay curves with the conducting glass electrode as the anode (+ electrode). In reading the curves in the bottom quadrant from left to right the decending trace represents the rise curve and the ascending trace the decay curve.

On the basis of these curves rise times (τ_R) and decay times (τ_D) can be calculated at the various wavelengths. They are given in Table VII. The rise time variation with wavelength is illustrated in Plate G. The results show rather long rise times, due to the low level of ambient lighting (10^{11}-10^{12} quanta/cm^{2}sec). There is no variation in rise and decay times with polarity. However, there appears to be a slight variation in the rise time with wavelength, the longest rise time being in the vicinity of 5350Å.

We have also made rise and decay time measurements using a single-crystal cell between two conducting glass electrodes. The thickness of this cell was 0.5mm. The incident wavelengths on both sides were the same, $\lambda_1 = \lambda_2 = 5200$Å. Masks were used to define exactly opposing spots. Iris shutters in front of each beam were connected to the same actuator in such a way that either shutter could be opened alone or both shutters opened simultaneously. A DC voltage of 15 volts was applied across the cell. Plate F shows the effect of

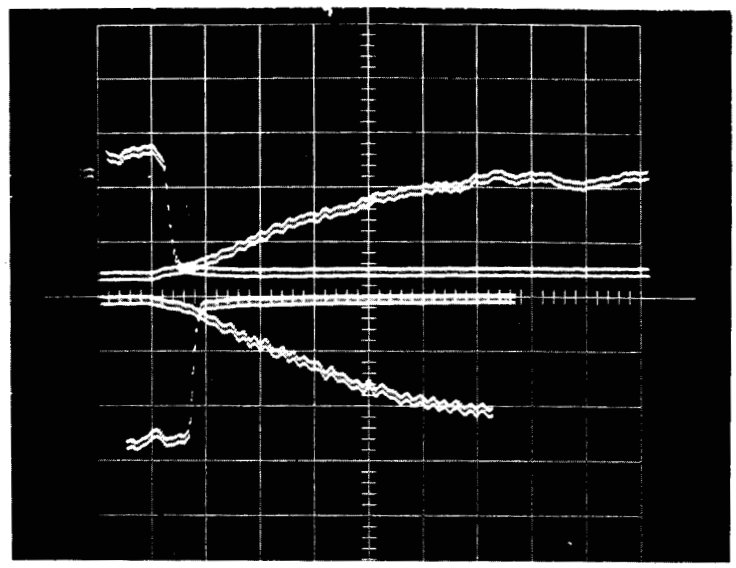

Signal (arbitrary units)

t (0.5 sec/div)

PLATE A = 5400Å

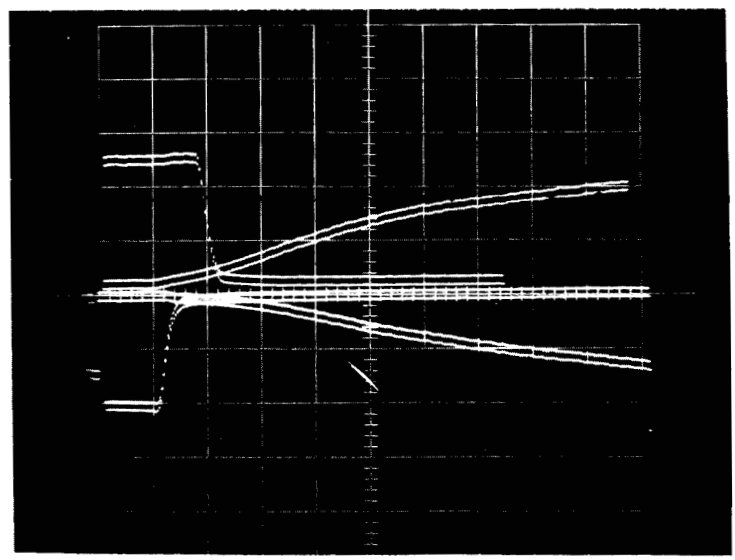

Signal (arbitrary units)

t (0.5 sec/div)

PLATE B = 5350Å

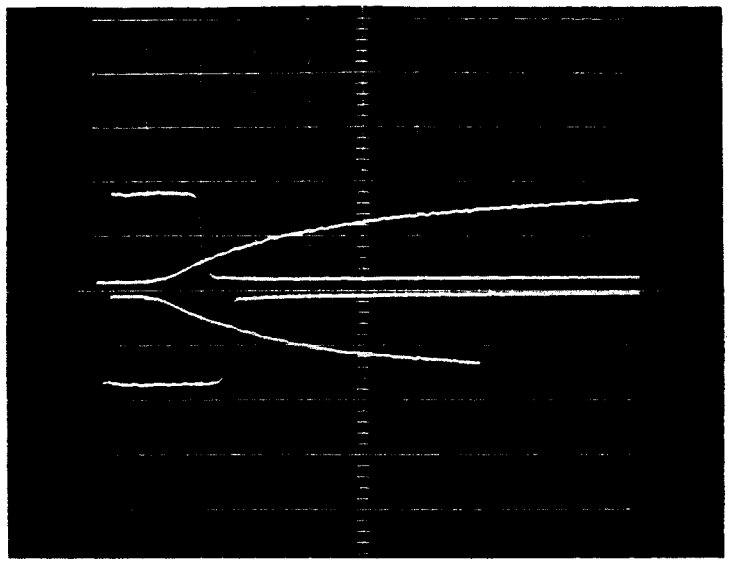

Signal (arbitrary units)

t (0.5 sec/div)

PLATE C = 5300Å

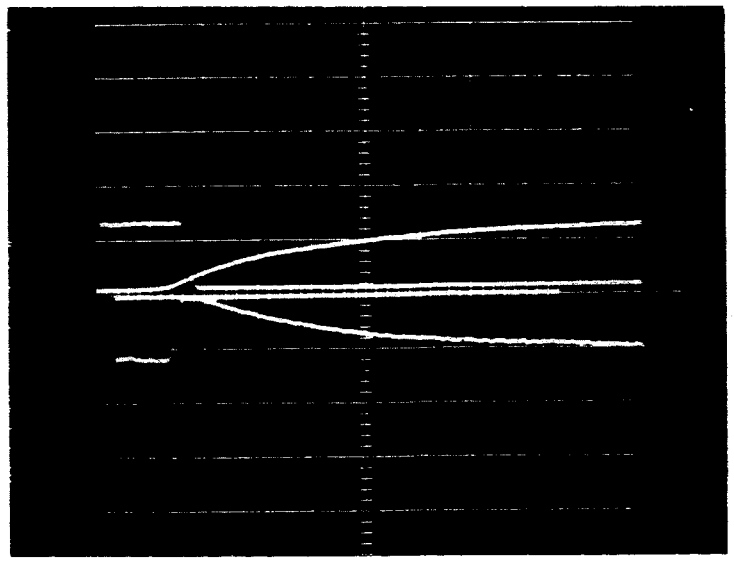

Signal (arbitrary units)

t (0.5 sec/div)

PLATE D = 5200Å

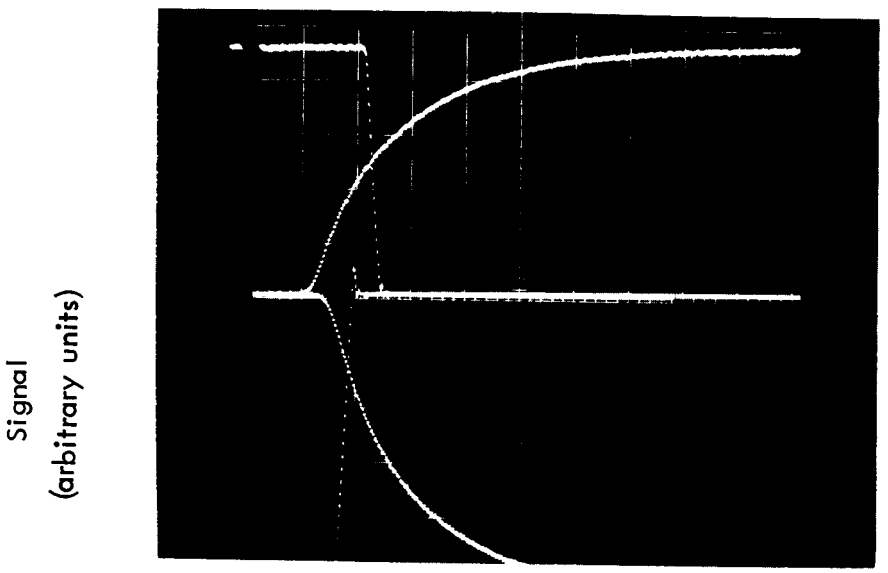

t (0.5 sec/div)

PLATE E = 6680Å

TABLE VII

RISE AND DECAY TIMES OF PHOTOCURRENTS

	Glass Electrode (-)		Glass Electrode (+)	
λ (Å)	t_R(sec)	t_D(sec)	t_R(sec)	t_D(sec)
5200	0.75	0.08	0.75	0.08
5300	1.2	0.08	1.2	0.08
5350	2.0	0.08	2.2	0.08
5400	1.45	0.08	1.6	0.08
6680	0.50	0.05	---	---

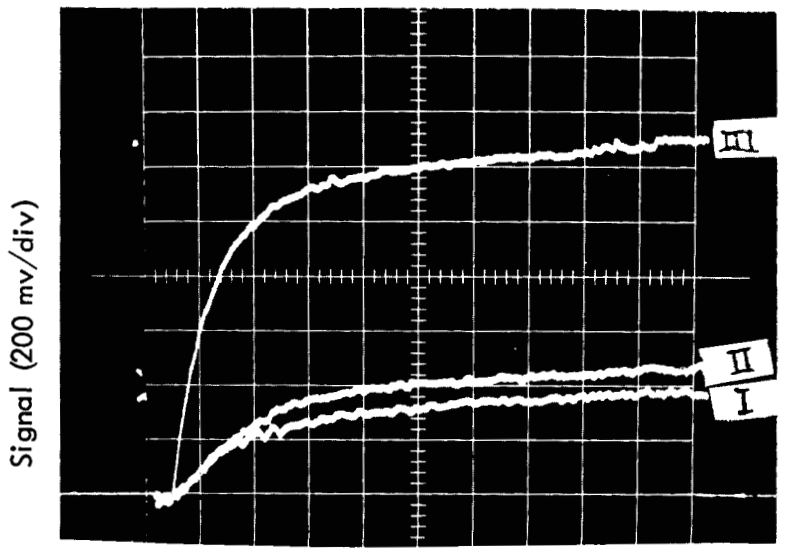

Signal (200 mv/div)

t (2 sec/div.)

PLATE F

V_{bias} = 15.0 volts

$\lambda_1 = \lambda_2$ = 5225Å

PLATE G. RISE TIME VARIATION WITH WAVELENGTH

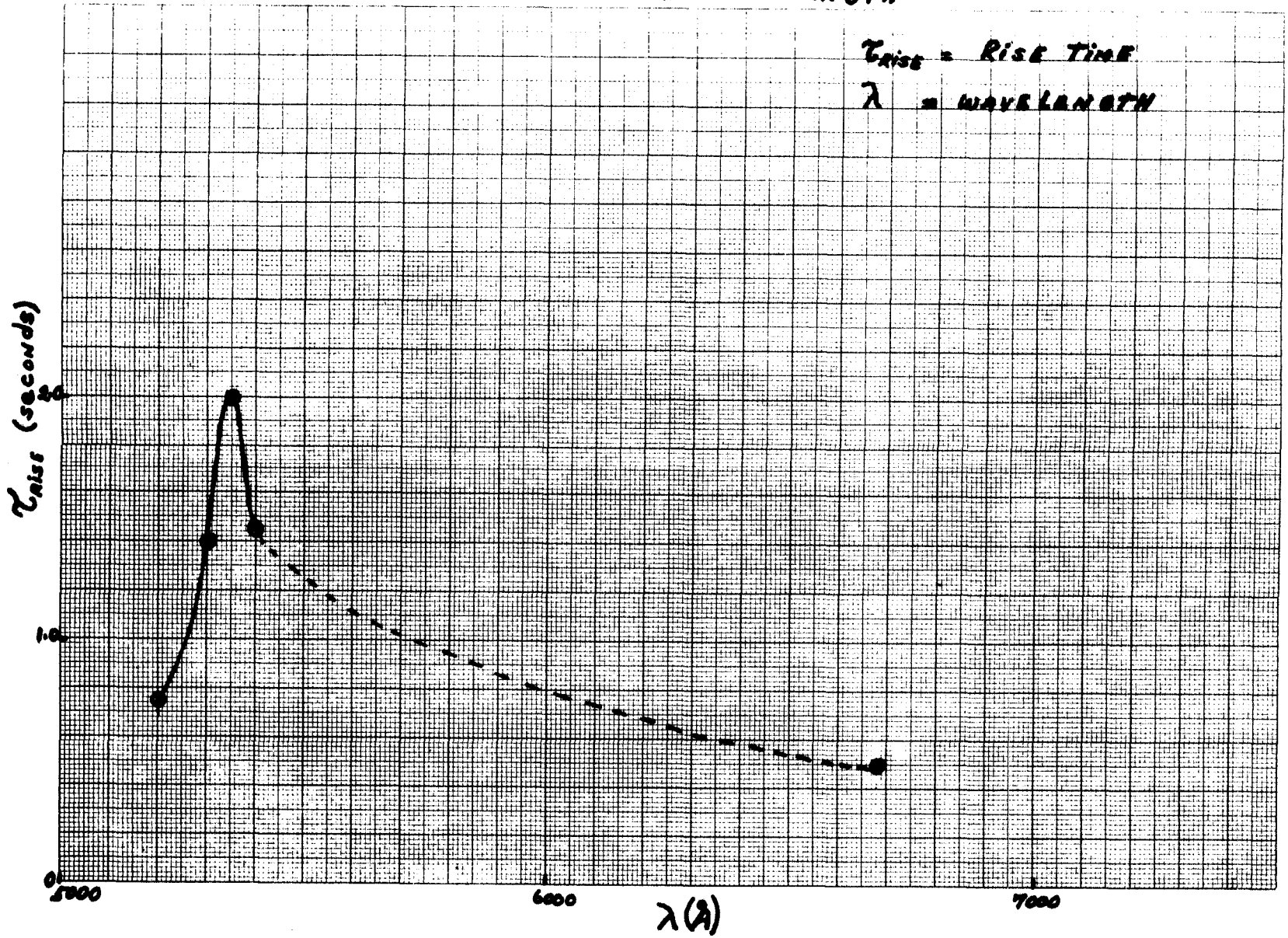

two-sided illumination on the rise time. The two lower curves show the current rise for one-sided illumination from either side, and the upper curve shows the rise of current when both beams are applied simultaneously. The vertical scale is the same for all three traces; the horizontal scale is 2 seconds per major division.

The calculated rise times are:

Curve I	2.0 sec
Curve II	2.2 sec
Curve III	1.2 sec

This experiment shows a considerable decrease in rise time when both sides are illuminated. While this is the only such experiment which we have made, we believe the results to be significant.

4. Geometrical Parameters

Several specialized experiments were performed in order to define the geometrical dependences of the multiplication effect. These included the normal versus acute angle illumination experiments, linear displacement of one beam relative to the other, and the simultaneous dual beam illumination of the same side of the photoconductor.

These experiments, performed under Item 4 of the work statement, serve to clarify the geometrical parameters governing the degree of multiplication and lay the foundation for a geometrical description of the effect.

a. Normal Versus Acute Illumination

In these experiments, we wished to determine whether the multiplication effect would be affected if the light impinged on the surface at an angle other than normal. An experimental arrangement which permitted varying the angle of incidence was therefore constructed. In order to insure that only the angle of incidence was changing, i.e. no linear displacement of either light spot was occurring, we used a General Electric diffractometer table, containing a goniometer which could rotate through 180°. Its axis of rotation could be very precisely located. The geometry of the experiment is presented in Figure 9. Two monochromators were used to supply the incident beams. One was mounted on the fixed portion of the table, while the other was mounted on the goniometer. Light spots were produced by using a microscope objective

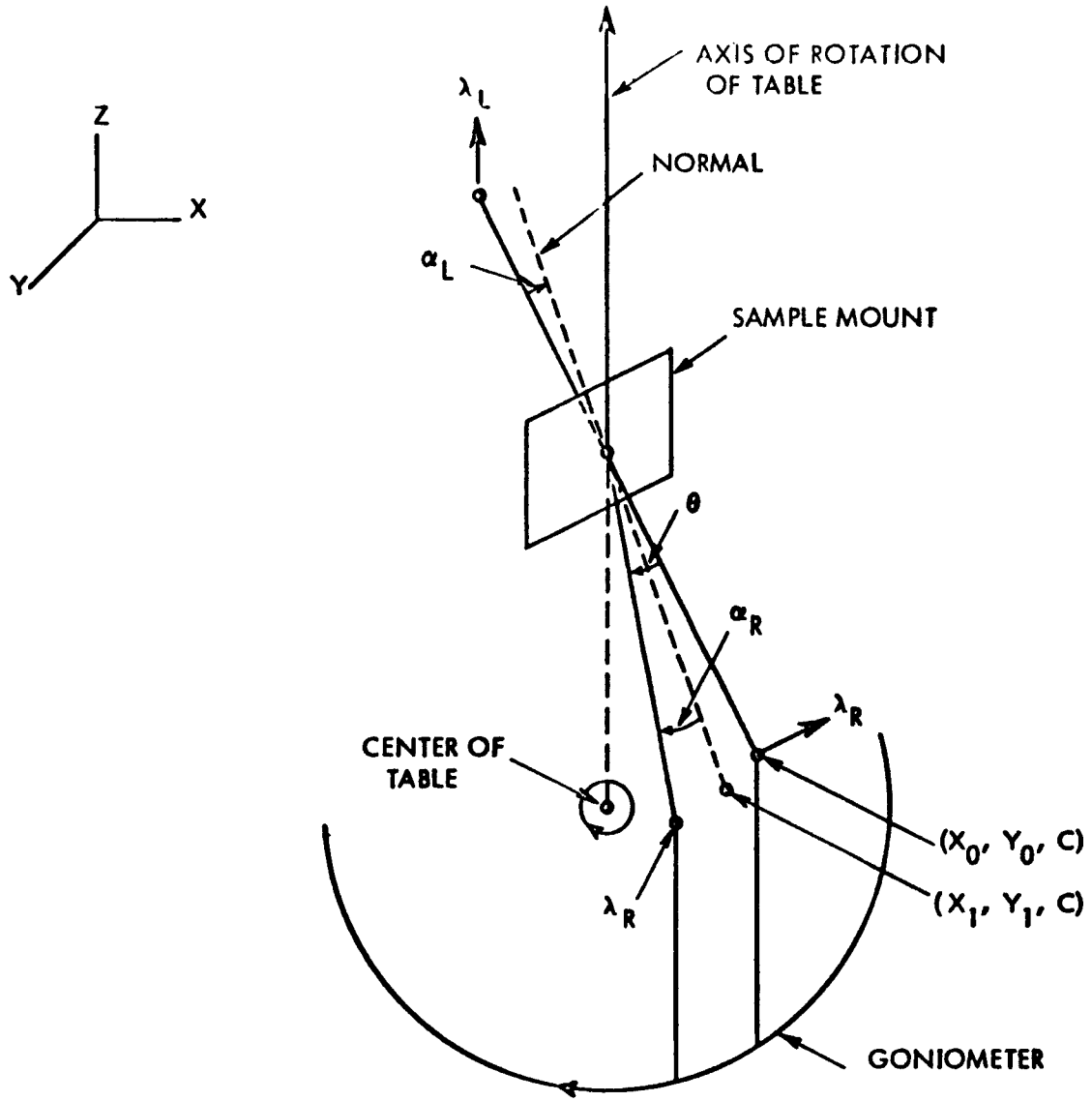

$\alpha_L \cong \alpha_R$ = ANGLE OF INCIDENCE

(X_0, Y_0, C) = INITIAL CO-ORDINATI OF NORMAL

(X_1, Y_1, C) = SUBSEQUENT CO-ORDINATES OF NORMAL

λ_L = FIXED MONOCHROMATOR

λ_R = MOVABLE MONOCHROMATOR

BEAM ANGLE VARIATION -
SCHEMATIC DIAGRAM OF EXPERIMENTAL ARRANGEMENT

FIGURE 9

lens and eyepiece combination. The area of each spot thus produced was very small compared to the surface area of the photoconductor. The sample mount was placed about 25 cm above the center of the table with the vertical axis of the table running precisely along the plane of the cadmium sulfide surface. The effect of moving the goniometer by an angle Θ was to rotate the sample mount by $\Theta/2$ and the moving monochromator by Θ, producing $\alpha_L = \alpha_R = \Theta/2$. ($\alpha_L$ is defined as the angle between the beam from the fixed monochromator and the plane normal to the sample, and α_R refers to the angle between the moving monochromator and the plane normal to the sample). A frosted glass surface was substituted for the CdS for the purpose of beam alignment and the spots from the two monochromators were made coincident for all values of Θ. This shows that the sample was truly on axis and the beams were truly radial. The approximate equality of α_L and α_R was established by setting the goniometer at zero ($\alpha_R \neq 0$) and then visually setting $\alpha_L \neq 0$.

First of all various wavelength combinations were tried in order to determine a set which gave a reasonable multiplication factor. Multiplication factors of 18.9 and 46.1 respectively were obtained when the combinations $\lambda_L = 5200\text{Å}$, $\lambda_R = 5800\text{Å}$, and $\lambda_L = \lambda_R = 5800\text{Å}$ were used at $\alpha_L = \alpha_R \cong 0$. The results of varying the angle of incidence are tabulated in Tables VIII- A and VIII- B.

An examination of the results in each of these tables shows that there is no dependence of the multiplication effect on the angle of incidence. The small decrease in the M factor noted in Table VIII- A can be explained by a small error in aligning the two light spots. The lack of a similar effect in Table VIII- B makes this explanation more probable than one based on a true angle effect.

In another experiment the surface of the photoconductor was displaced from the axis of rotation by placing a spacer between the photocell holder and the sample mount. The results of this experiment are tabulated in Table VIII- C. It can be seen from this table that the rate of decrease of M with angle is much larger than in the results presented in the two preceding tables. This is to be expected with a linear displacement of the two light spots, and confirms the explanation of the Table VIII- A results given in the previous paragraph.

On the basis of the results presented above we conclude that the multiplication effect is independent of the angle of incidence of the respective light beams. This means that it is not necessary that the two beams

TABLE VIII

EFFECT OF BEAM ANGLE ON M

A.

$\lambda_L = 5200\text{Å}$ $\lambda_R = 5800\text{Å}$ V=1.5 volts

Angle of incidence (degrees) ($\alpha_L = \alpha_R$)	i_L	i_R	i_T	M
		$\times 10^6$ (amps)		
0	.01	7.91	150	18.9
2.5	.01	7.9	145	18.3
5.0	.01	7.9	145	18.3
7.5	.01	8.3	145	17.5
10.0	.01	8.2	140	17.1
12.5	.01	8.1	138	16.8
15.0	.01	7.8	129	16.5
17.5	.01	7.6	120	15.8
20.0	.01	7.7	115	14.3
22.5	.01	7.7	108	14.0
25.0	.01	7.4	92	12.4
27.5	.01	6.5	88	13.5

i_L = photocurrent from left monochromator (λ_L) alone.
i_R = photocurrent from right monochromator (λ_R) alone.
i_T = total photocurrent produced when photocell is simultaneously illuminated by both monochromators.
M= multiplication factor.

TABLE VIII (Continued)

B.

$\lambda_L = \lambda_R = 5800$Å

V=1.5 volts

$\times 10^6$ (amps)

Angle of incidence (degrees) ($\alpha_L = \alpha_R$)	i_L	i_R	i_T	M
0	1.70	6.55	380	46.1
2.5	1.70	6.55	380	46.2
5.0	1.40	6.60	370	44.6
10	1.35	6.50	360	46.8
15	1.45	5.70	330	46.2
20	1.50	5.60	300	42.6
25	1.50	4.80	275	43.7
0	1.60	6.80	375	45.2

C.

$\lambda_L = 5200$Å $\lambda_R = 5800$Å V=1.5 volts

0	0.01	10.9	185	17.0
2.5	0.01	13.9	119	8.6
5.0	0.01	13.9	102	7.3
7.5	0.01	13.4	81	6.0
10.0	0.01	12.8	70	5.5
12.5	0.01	11.8	58.4	5.0
15.0	0.01	11.2	51	4.6
17.5	0.01	10.9	44.5	4.1
20.0	0.01	10.4	39.9	3.8
22.5	0.01	10.4	34.9	3.4
25.0	0.01	8.9	31.9	3.6
27.5	0.01	7.0	24.4	3.5

be co-linear. Of course, the effect only occurs when the two light spots are directed to the same area on opposite surfaces.

b. Effect of Relative Displacement of the Light Spots

The multiplication effect is observed when two light beams are directed to exactly opposing spots on the opposite surfaces of the photoconductor. When the two light spots are incident on different points on the two faces there is little or no enhancement of the photocurrent (M=1). The object of this phase of the study was to determine quantitatively how the linear displacement of the two light beams affect the multiplication factor. In these experiments the position of one of the light spots was permanently fixed and the other spot was systematically displaced.

One spot of radius 0.4 mm and one spot of radius 0.2 mm were employed. In order to carry out these experiments, the light spots first had to be made to coincide precisely. To accomplish this, a frosted glass plate was inserted in the path of the light beams emanating from each monochromator. Each beam was focused onto the glass plate by means of a microscope objective - eyepiece lens combination. The two beams were visually centered as well as possible. The use of an auxiliary magnifying lens enabled us to secure complete overlap of the two light spots. After the two light spots were made to coincide, the photoconductive cell in an appropriate holder was inserted in place of the frosted glass plate and M was determined for various positions of the moving beam.

The displacement of one of the light spots was effected by inserting a glass plate of 3.0 mm thickness in the path of the beam. As long as the glass plate is normal to the beam, there is no displacement. When the plate is rotated by an angle α, the beam is displaced, without change of direction, by a distance X:

$$X = d \sin\alpha \left(1 - \sqrt{\frac{1 - \sin^2\alpha}{n^2 - \sin^2\alpha}}\right)$$

where n is the refractive index of the glass with respect to air, measured as 1.52, and d is the thickness of the plate. The glass plate was mounted on a large piece of cork which had been centered on a protractor. Angles were read to better than 0.5°. By rotating the glass plate up to 70° in each direction, displacements up to 2.0mm were obtained. The results of these measurements are given in Figure 10. They indicate that the displacements were large enough to reduce M nearly to unity. Considerable difficulties were encountered in these

experiments because the requirements for dimensional stability were severe. However, the results shown in Figure 10 were adequately reproducible.

c. Simultaneous Dual Beam Illumination of a Single Surface

The possibility that multiplication phenomenon could be produced by simultaneous dual-beam illumination of a single surface of the photoconductor was also investigated. Again masks were employed. Simultaneous illumination of the same side was accomplished by placing the bias source at right angles to the variable excitation source with a prism beam splitter being inserted in the two light paths. This accurately superimposed the bias radiation beam on the axis of the variable excitation source. The combined beam was then focused onto the photoconductor.

The results of this experiment are presented in Figure 11, where once again the bottom curve represents the response of the cell with the bias source off and the subsequent curves represent the response of the source with the bias source on and the variable excitation source off. The numbers above each curve are the current obtained when only the bias source was on. This figure should be compared with Figure 5. It is obvious that no multiplication occurs and that it cannot be obtained in this geometrical arrangement by varying either the wavelength of one source or the intensity of the other.

d. Effect of Varying Wavelength

This topic has been reported on under item 3a.

e. Effect of Varying Spot Size.

This topic has been reported on under item 3a.

FIGURE 10 . Effect of Linear Displacement on M.

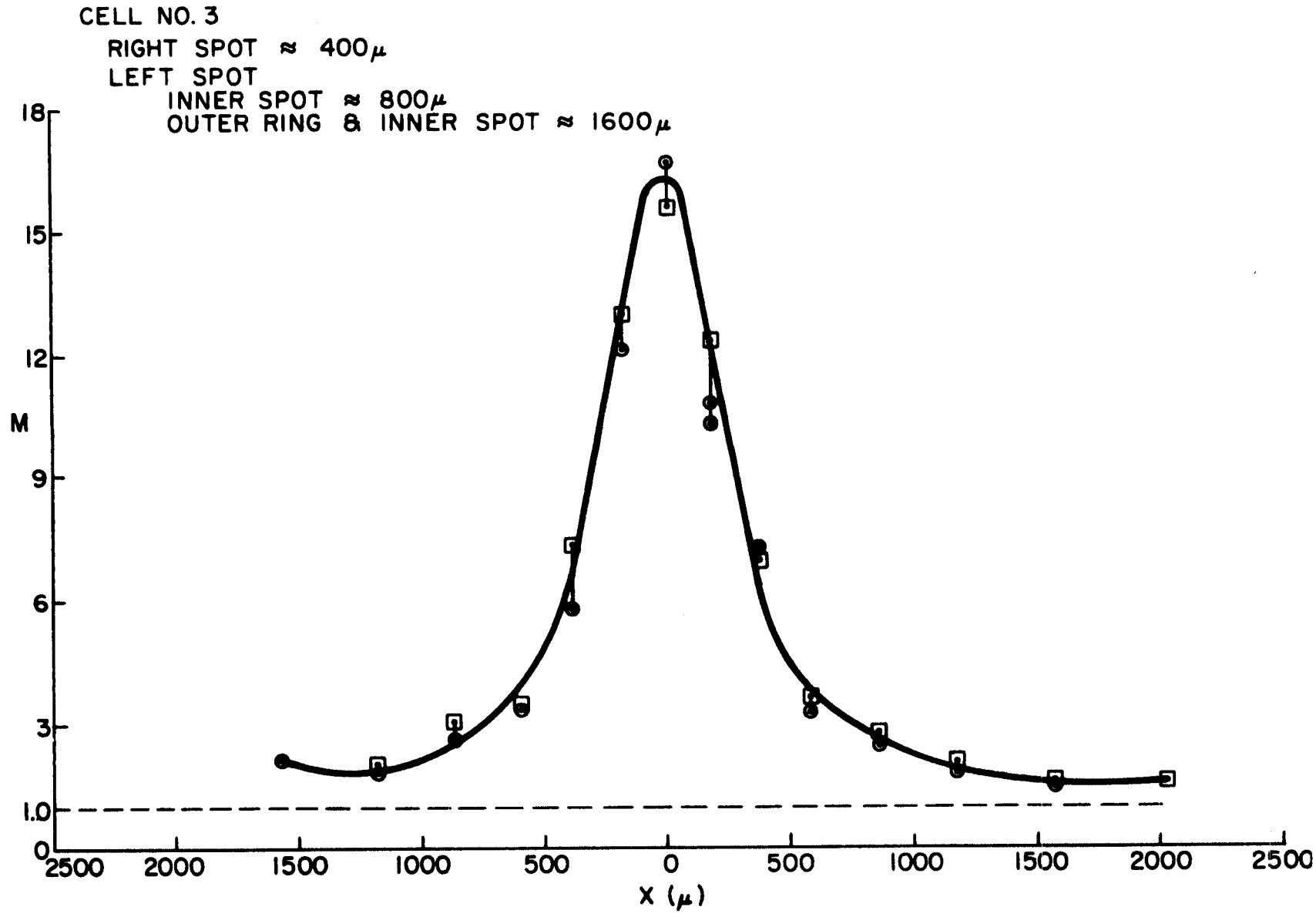

FIGURE 11

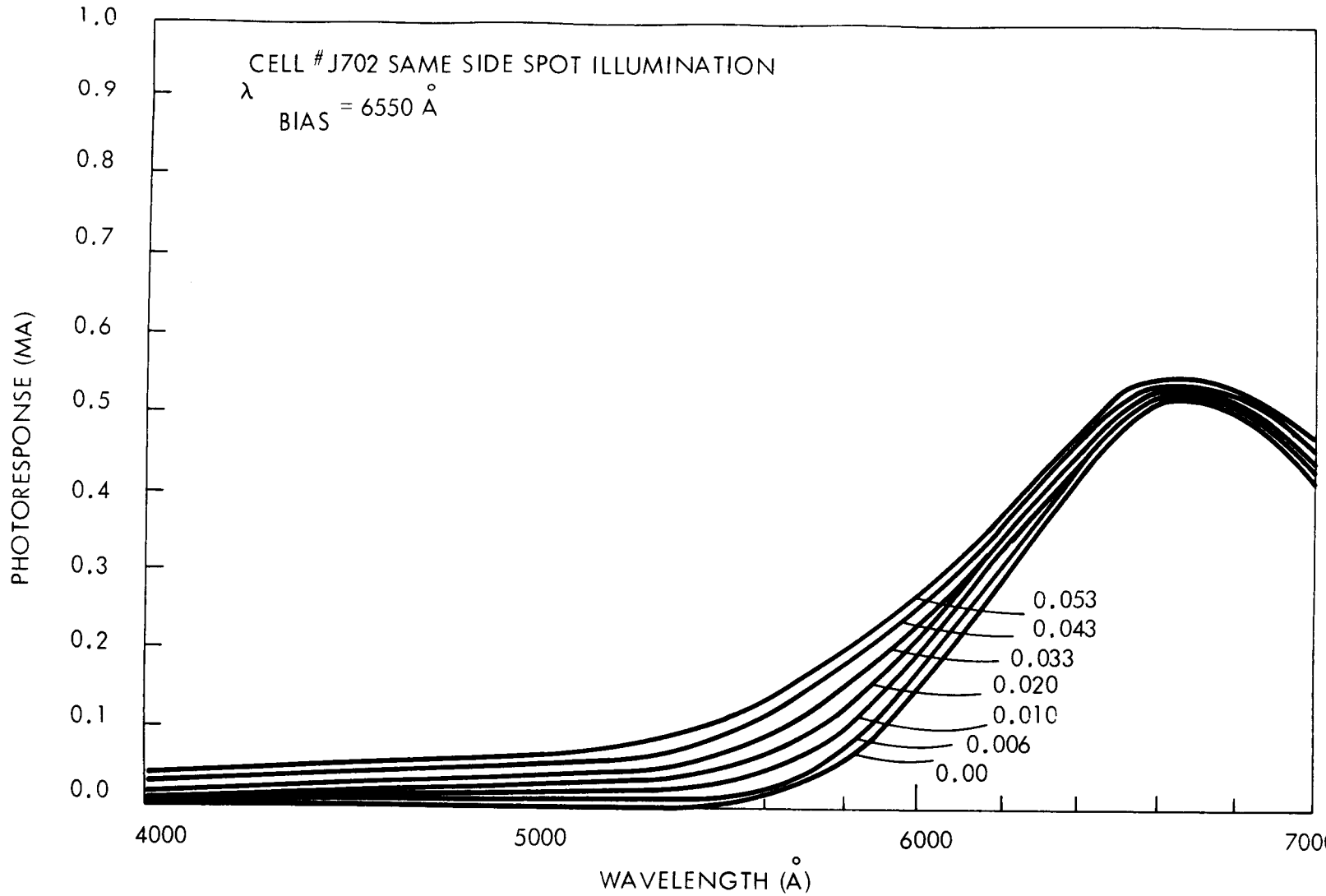

VARIATION IN PHOTORESPONSE CURVE FOR SEVERAL INTENSITIES OF BIAS ILLUMINATION
(NUMBERS OVER CURVES GIVE CURRENT (MA) DUE TO BIAS ILLUMINATION ALONE)

III. THEORY OF THE MULTIPLICATION EFFECT

1. Introduction

In this section we present some approaches to a theoretical description of the multiplication effect. It is evident, first of all, that the geometry of the system is of prime importance. Small changes in the geometry of the experiment cause large changes in the observed photocurrents, and indeed this is what gives the multiplication effect its potential practical value. One therefore tends to try at first for a purely geometrical explanation of the effect, and such an explanation is not hard to find.

One quantitative treatment is demonstrated in the attached diagrams. The argument is as follows. Since the conduction is ohmic, the observed current is inversely proportional to the resistance of the photoconductor. The resistance, in turn, is the sum of the resistances of the various layers. When illumination is from one side only (Figure 12), charge carriers are generated only on that side and the concentration of charge carriers diminish in a regular fashion. A high-resistance region will remain near the other side. However, when both sides are illuminated, the overlap of the penetration curves (Figure 13) is such that there is no longer a region of very high resistance. Thus the total current can be much higher. If there is a good deal of lateral diffusion of charge carriers (normal to the field direction), this effect will be much more marked when small areas are illuminated than when large surfaces are illuminated.

It is, however, easy to show that there is more to the effect than simple geometry. This can be seen from the wavelength dependence of the multiplication effect. In polycrystalline cadmium sulfide, for instance, the greatest value of the multiplication factor is usually achieved when the impinging wavelengths are 5200Å from one side and 6500Å from the other side. Now light of 6500Å by itself does produce carriers and give a measurable photocurrent; but light of 5200Å wavelength by itself gives virtually no photoconductivity. It is therefore clear that the multiplication effect cannot be explained simply by adding the concentrations of charge carriers produced by the two beams in each volume element of the photoconductor; for in this case the 5200Å beam adds none. A more subtle effect is evidently present, and consideration of the physics of the photoconductor is required. We shall treat the geometrical and physical factors separately, since our efforts at model building have not yet reached the point at which it is profitable for us to combine them.

2. Geometrical Models of the Multiplication Effect

a. First Crude Model

FIGURE 12.

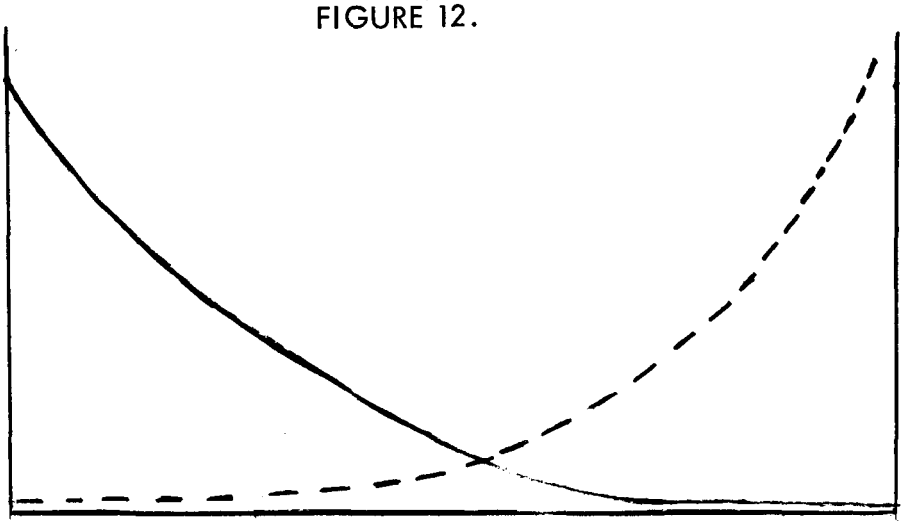

Left-hand illumination
Full line: charge carrier concentration as a function of depth (arbitrary units).
Broken lines: local electrical resistance as a function of depth (arbitrary units).

FIGURE 13.

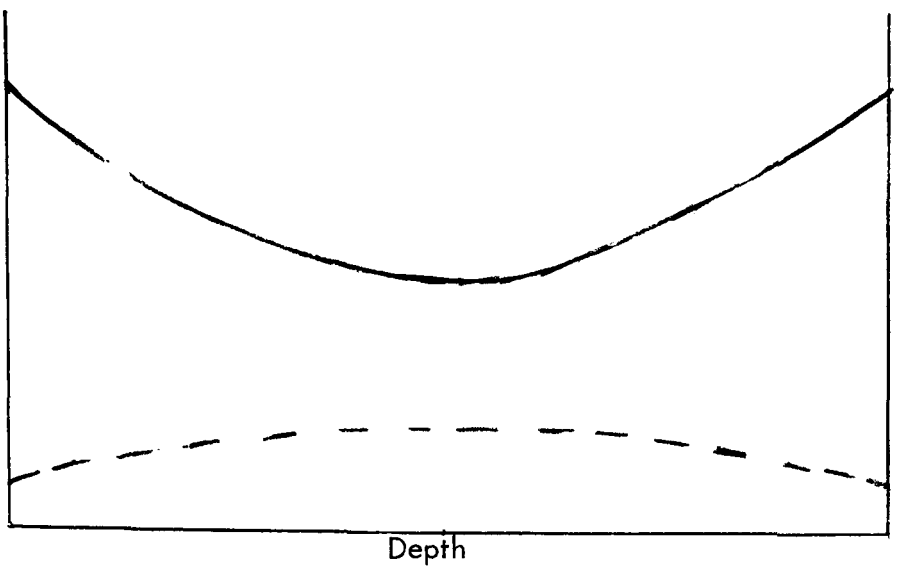

Illumination from both sides
Functions same as in Figure 12.

We start with a very crude model which nevertheless has some interesting features. First of all, the model is one dimensional. We assume to a first approximation that the concentration of carriers is invariant in the direction normal to the field. We justify this by noting that in these experiments the spot size is greater than the thickness of the photoconductor and that the major conduction path is the most direct path between the spots; but the results of the spot displacement experiments indicate that such a view is oversimplified. Secondly, we consider the photoconductor as being divided into several equally thick regions (layers), each of which is treated as if it contains uniform carrier concentrations. As one moves away from the illuminated surface, each layer has a carrier concentration which is n times that of the previous layer ($n < 1$).

If only one side is illuminated and we arbitrarily divide our photoconductor into three layers, these layers will have carrier concentrations of 1, n, and n^2 respectively (the concentration in the illuminating layer being taken as our unit of concentration). The resistances of the layers are, respectively:

$$k,\ k/n,\ k/n^2$$

(k is a proportionality constant)

The total resistance is

$$R = k(1+\frac{1}{n} + \frac{1}{n^2}) = k\,\frac{n^2+n+1}{n^2}$$

and the photocurrent

$$i_1 = \frac{V}{R} = \frac{V}{k}\qquad \frac{n^2}{n^2+n+1}$$

The photocurrent i_2, with the other side illuminated, is exactly the same.

When both sides are illuminated, the carrier concentrations are presumed to be the sums of those attributable to each light source alone:

$$1+n^2,\ 2n,\ 1+n^2$$

$$R = k\,(\frac{1}{1+n^2} + \frac{1}{2n} + \frac{1}{1+n^2}) = \frac{k(n^2+4n+1)}{2n(n^2+1)}$$

$$i_T = \frac{E}{k} \quad \frac{2n(n^2+1)}{n^2+4n+1}$$

The multiplication factor is

$$M = \frac{i_T}{i_1+i_2} = \frac{2n(n^2+1)\ (n^2+n+1)}{2n^2(n^2+4n+1)} = \frac{(n^2+1)\ (n^2+n+1)}{n(n^2+4n+1)}$$

$$M = \frac{1+n+2n^2+n^3+n^4}{n+4n^2+n^3}$$

We see that for n = 1, M = 6/6=1, as it should For $n \longrightarrow 0$, $M \longrightarrow 1/n$.

There is a deviation function F=1-Mn(i.e.$M=\frac{1}{n} - \frac{F}{n}$) which is zero at n=1 and n=0 and positive at all values in between. Its maximum is at n=0.37, F=0.345. Some other values of F are:

n = 0.9	F = 0.103
0.5	0.327
0.1	0.205
0.01	0.029

Applying this model to our values, we see that a value of the multiplication factor M=85 would correspond to n=0.011. (M=8 gives n=0.1).

$$0.011 = e^{-4.5}$$

$$0.1 = e^{-2.3}$$

It would then follow that the e-folding distance for carrier concentration in the photoconductor would be one-fifth to one-tenth of the conductor thickness or about 10 microns. But it is necessary to go to a better model before a more definite conclusion can be drawn.

The merit of this very crude model is that it shows, without complicated mathematics, how the multiplication factor can originate.

b. Second Geometrical Model

We are now ready to go to a second geometrical model which will do much the same thing in a more sophisticated way. This will still be a one-dimensional model. The photoconductor is supposed to be almost opaque so that all the carriers are generated in an infinitesimal surface layer in which a steady-state concentration C_o is maintained. Carriers diffuse out and are also affected by recombination with traps or recombination centers (whose concentration is assumed uniform and constant) and by the electric field E. The photoconductor thickness (in the x direction) is d.

The equation governing the concentration of the carriers is then

$$\frac{\partial C}{\partial t} = 0 = D \frac{\partial^2 C}{\partial x^2} - kC - \mu E \frac{\partial C}{\partial x}$$

D - diffusion constant (cm^2/sec)
k - recombination constant (sec^{-1})
μ - charge carrier mobility (cm^2/volt-sec)

It is assumed here that the field is moving the carriers away from the illuminated surface; since there is reason to believe that practically all the current is carried by electrons, this equation applies to illuminating the negative electrode.

The boundary conditions are $C(0)=C_0$, $C(\infty)=0$, and the solution is

$$C=C_0 \exp \left[\frac{x \mu E}{2D} \left(1 - \sqrt{1+ \frac{4kD}{\mu^2 E^2}}\right)\right];$$

for $4kD << \mu^2 E^2$, this reduces to:

$$C=C_0 \exp (-kx/\mu E)$$

In a layer of thickness dx, the resistance will be proportional to dx and inversely proportional to C.

$$dR = \frac{M\ dx}{C_0 \exp\left[\frac{x\mu E}{2D}\left(1-\sqrt{1+\frac{4kD}{\mu^2E^2}}\right)\right]}$$

$$R = \int_0^d dR = \frac{M}{C_0}\int_0^d \exp\left[-\frac{x\mu E}{2D}\left(1-\sqrt{1+\frac{4kD}{\mu^2E^2}}\right)\right] dx$$

$$= \frac{2MD}{C_0\mu E\left(1-\sqrt{1+\frac{4kD}{\mu^2E^2}}\right)}\left\{\exp\left[-\frac{\mu Ed}{2D}\left(1-\sqrt{1+\frac{4kD}{\mu^2E^2}}\right)\right]-1\right\}$$

$$i_1 = \frac{V}{R} = \frac{Ed}{R} = \frac{E^2 d\,\mu C_0\left(1-\sqrt{1+\frac{4kD}{\mu^2E^2}}\right)}{2MD\left\{\exp\left[-\frac{\mu Ed}{2D}\left(1-\sqrt{1+\frac{4kD}{\mu^2E^2}}\right)\right]-1\right\}}$$

For the current in the reverse direction we have a similar equation except that the sign of the field term is reversed. We shall allow a different illumination intensity, giving a steady state concentration C'_0 at the surface.

$$\frac{\partial C'}{\partial t} = 0 = D\frac{\partial^2 C'}{\partial x^2} - kC' + \mu E\frac{\partial C'}{\partial x}$$

Boundary conditions: $C'(d) = C'_0$, $C'(-\infty) = 0$

The equation has the solution

$$C' = C'_0 \exp\left[-\frac{\mu E(d-x)}{2D}\left(1-\sqrt{1-\frac{4kD}{\mu^2E^2}}\right)\right]$$

and by a similar evolution we obtain

$$i_2 = \frac{E^2 C_0' \mu d \left(1 - \sqrt{1 - \frac{4kD}{\mu^2 E^2}}\right)}{2MD\left\{\exp\left[\frac{\mu E d}{2D}\left(1 - \sqrt{1 - \frac{4kD}{\mu^2 E^2}}\right)\right] - 1\right\}}$$

When both sides are illuminated, we have

$$C_T = C + C'$$

$$= C_0 \exp\left[\frac{\mu E x}{2D}\left(1 - \sqrt{1 + \frac{4kD}{\mu^2 E^2}}\right)\right] + C_0' \exp\left[\frac{\mu E (d-x)}{2D}\left(1 + \sqrt{1 - \frac{4kD}{\mu^2 E^2}}\right)\right.$$

$$i_T = \frac{Ed}{\left| \int_0^d \frac{M\,dx}{C_T} \right|}$$

It appears that an analytical solution of the integral $\int \frac{dx}{C_T}$ may be possible. This would immediately give us an analytical expression for the multiplication factor M in this model. However, the integral has not yet been solved.

A solution has, however, been obtained for the high-field case $4kD \ll \mu^2 E^2$. In this case we can apply the approximation

$$\sqrt{1 + 2a} = 1 + a \quad (|a| << 1)$$

This gives

$$C = C_0 \exp\left(-kx/\mu E\right)$$

$$C' = C_0' \exp\left[-k(d-x)/\mu E\right]$$

The multiplication factor turns out to be:

$$M = \frac{\sqrt{C_0 C_0'}}{E(C_0 + C_0')} \frac{\exp\left(kd/2\mu E\right) - \exp\left(-kd/2\mu E\right)}{\arctan\left(\left[\frac{C_0}{C_0}\right]^{1/2} \cdot e^{kd/2\mu E}\right) - \arctan\left(\left[\frac{C_0'}{C_0}\right]^{1/2} \cdot e^{-kd/2\mu E}\right)}$$

It will be noted that at high fields the multiplication factor decreases with increasing E. This is in agreement with observation.

3. Physics of the Multiplication Effect

As discussed above (page 51), the first thing that any theory of the multiplication effect should explain is the ability of light which does not itself produce photoconductivity to augment the photocurrent produced by another light source. Also, the theory must, of course, ultimately account for and predict the effect of field, light intensity, spot size and the material parameters.

The phenomenon may well be allied to the general phenomenon of sensitization in photoconductors as developed by Albert Rose ("Concepts in Photoconductivity and Allied Problems," Interscience, New York, 1963, pp. 43-47).

Rose's description relies on the presence of two kinds of recombination centers. One, which is also present in the unsensitized material, has roughly equal capture cross-sections for electrons and holes. The other, present in the sensitized material only, has a normal capture cross-section for electrons. When recombination centers of the second kind are present, they will therefore be almost entirely populated by holes. To preserve electrical neutrality, the centers of the first kind will be almost entirely populated by electrons, and will thus lose their ability to capture electrons. Since the electrons cannot then be captured by centers of either kind, their mean free path and hence their mobility will be increased over the values in the unsensitized material, so that an equal number of light-generated electrons can carry a much higher current. The net result is a sensitized photoconductor.

We may consider how such an explanation could apply to our experiments. It is evident that the production of charge carriers by 6500Å light is due to the promotion of electrons from recombination centers to the conduction band. (Not from the broad valence band, because the more energetic 5200Å quanta do not produce the charge carriers). We postulate that the 5200Å light produces the traps of the second kind near the unilluminated surface. The number of charge carriers in the vicinity of the unilluminated surface would remain small, but, as a result of the formation of centers of the second kind, their mobility would increase, so that the resistance of this region would be lowered.

We may ask how this model can be reconciled with the geometrical model of the previous section. The centers of the second kind may be viewed as virtual charge carriers, since their appearance makes each of the charge carriers as effective in carrying current as several charge carriers would be in their absence. It is therefore correct, in a formal geometrical model, to treat them as actual charge carriers.

Some change would, however, be required because the parameters of the actual charge carriers (free electrons) and the virtual charge carriers would not be the same. This applies particularly to the diffusion constant D (presumed to be smaller for the recombination centers), the electrical mobility and the recombination constant k. Thus, while the same differential equation and boundary conditions would apply, the steady-state distribution of the virtual charge carriers could be quite different than that obtained for electrons.

An extreme case would be the assumption $D=0$, $\mu=0$. This implies that the recombination centers are completely immobile. The lowering of resistance through finite layers of photoconductor would indicate that they are not all on the surface; but such a distribution could be accounted for by taking a finite extinction coefficient for the light. The concentration of recombination centers at depth (d-x) would then be given by

$$C=C_0 \quad \exp\ (d-x)\ E,$$

which has the same form as the expressions previously derived, but is not field-dependent.

It therefore seems that an interpretation along sensitization lines is compatible with the geometric models.

IV. CONCLUSIONS AND RECOMMENDATIONS

1. Conclusions

It is of interest to summarize at this point what is known about the multiplication effect in semiconductors as a result of this research effort. First of all, it has been confirmed that the effect is real, that it is potentially useful, both as a beam alignment tool and for other uses, and that it cannot as yet be fully explained.

It appears to be an essential feature of our experiments, at least insofar as they relate to polycrystalline doped CdS cells, that the optical extinction coefficient of the cells is very high, so that light is absorbed near the surface. This observation suffices to explain completely the lack of dependence of the multiplication effect on the angle of incidence of the light beam (item 4a). If the effective path of the beam inside the photoconductor is negligibly short (e.g. much smaller than the spot radius), then it does not matter what its direction is.

High light absorption also suffices to explain the failure to observe the multiplication effect when both beams illuminate the same side of the photoconductor. If the extinction coefficients were of the order of 50 cm^{-1} as in pure CdS, so that one or both of the beams could pass through these thin photoconductors with little attenuation, it would be unlikely to have so marked a difference between opposite-side and same-side illumination. The observed absorption is so intense that the light from each beam is almost entirely absorbed very near the surface on which it falls; under these circumstances, the observed contrast between the two modes of illumination could be explained.

Of course, the high extinction coefficient in itself is not enough to explain the effect. The geometrical models of section III.2 represent an attempt to explain it further.

Several of the other experiments are also germane to the diffusion model. One of these is the linear displacement of the spots relative to each other. It is of interest to find out whether the curve of M as a function of this displacement can be accounted for by the overlap of the light spots or whether it requires the assumption of lateral diffusion of the charge carriers. Table IX is a comparison of observed values of M and the values calculated on the basis that multiplication only occurs in areas of spot overlap. The table shows that the multiplication effect persists even when the light spots no longer overlap. This is another powerful support for the validity of a geometrical diffusion model.

On the other hand, the dependence on wavelength cannot be adequately explained by our geometrical model. We have attempted a physical explanation, which is given in section III, 3.

TABLE IX

COMPARISON OF ACTUAL AND CALCULATED M

a (mm)	M (Actual)	M (calculated)
0	16.7, 15.5	16.1 (average)
0.182	12.3, 13.0, 12.1, 10.8	16.1
0.374	7.25, 5.80, 7.37, 6.93	9.0
0.598	3.30, 3.33, 3.32, 3.65	1.1
0.862	2.86, 2.68, 2.50, 3.09	1
1.180	1.87, 1.89, 2.03, 2.07	1
1.570	1.48, 2.18, 1.59	1
2.035	1.57, 1.57	1

Our conclusion from the available evidence is, therefore, that, while no complete theoretical explanation of the multiplication phenomenon is yet available; considerable insight into its nature has been obtained. Both diffusion and something akin to sensitization must be taken into account for a complete explanation.

An important consequence of the physical model is that the multiplication phenomenon is a function of certain material parameters related to the nature of the matrix and the process of sensitization. Since sensitization is not a property of all photoconductors there is, therefore, less reason to expect that the effect will be observed in all materials.

The dependence of the multiplication effect on applied field seems to be adequately explained by our geometrical model. The intensity dependence is not yet explained.

2. Recommendations

The ultimate interest of General Precision and the U. S. Government is in practical applications of this effect. In addition to the beam alignment potential, many of the applications which we envisage involve the recognition of patterns, i.e. matching a projected pattern to a known pattern projected onto the other side of a photoconductor. The feasibility of such applications cannot be evaluated until we determine whether several pairs of light spots illuminating exactly opposite points on the two photoconductor electrodes, will also exhibit multiplication. At the present time there is every reason to believe that, if the distance between pairs of spots is more than 1-2 mm, their behavior will be completely independent. Experimental confirmation of this conjecture is required.

We are aware that the simple photoconductor cells fabricated in this laboratory have not performed as well as we had hoped and, consequently, progress on understanding material and dimensional dependences have been hindered. In particular, the influence of photoconductor thickness must still be characterized, especially for the evaluation of various models.

An important question about the multiplication effect which has not yet been answered is whether it is characteristic of cadmium sulfide alone or of many or all photoconductors. From our sensitization model it could be infered that it may be limited to CdS and related materials (e.g., CdSe), because only they show sensitization and supralinearity. On the other hand, the geometrical model would seem to apply to any photoconductor,

if only it is opaque enough. To resolve this question, it is necessary that experiments be performed with other photoconductors, such as lead sulfide and germanium, and that these experiments be, in the first instance, directed at establishing the presence and wavelength dependence of the effect. Eventually it will be desirable to perform, on each photoconductor for which the effect is found, the whole gamut of experiments which have already been done for cadmium sulfide; however, we regard the completion of this data-gathering effort as less urgent than the initial characterization of photoconductive multiplication.

The characterization of the effect in cadmium sulfide itself is incomplete, particularly insofar as its dependence on composition is concerned. The composition of the commercial photocells, in which the effect is most marked, is unknown and the cells prepared in this laboratory have been less than satisfactory. It is recommended that future research include the preparation of a series of cells of known composition, and an effort to optimize the multiplication effect parameter with respect to composition. It would be most desirable if suitably doped single-crystal cells were among those prepared.

So far, most of our experiments have involved steady-state illumination of the photoconductor. Now that we have reason to suspect that diffusion of charge carriers is important, it appears reasonable to initiate an investigation of time-dependent phenomena. The experiments envisaged involve the interposition of a periodic shutter (e.g. a rotating wheel with an empty sector) in each beam. In this way we can develop situations such as the following:

a. the two spots are illuminated alternately .
b. the spots are illuminated alternately, but there is an interval in which both or neither are on.
c. one is illuminated steadily while the other is periodic, etc.

The objective of these variations would be to determine the time required for the charge carriers (actual or virtual) from the two spots to interact, the time which may be required for the saturation of trapping states, and other kinetic parameters.

3. Recommended Program

We conclude this report by setting out a suggested research program which would, in our opinion, be suitable for implementation in the next 12-18 months. It will not be as broad as the recommendations of the previous section, since we do not think that a rate of effort sufficient to solve all problems simultaneously can be justified.

In our opinion, the immediate research program should contain the following tasks:

A. Again fabricate cadmium sulfide photoconductors with different thicknesses, all having the same composition, and determine the effect of thickness on the multiplication effect.

B. Fabricate effective photoconductors of cadmium sulfide with a variety of dopants and dopant levels, and determine the dependence of the multiplication effect on composition.

C. Extend the determination of rise and decay times of the multiplication effect and perform experiments involving periodic illumination of either or both sides.

D. Design, fabricate, and test a "breadboard" device utilizing the multiplication effect for beam alignment.

NASA-Langley, 1966 CR-431